

# An Insight to the Various Applications of Hydroxyapatite

Quentin Ray Tjiah Lim<sup>1</sup>, Xin Yi Cheng<sup>2</sup>, Chien Yi Wee<sup>3,\*</sup>

<sup>1</sup>Department of Materials Science and Engineering, National University of Singapore, Singapore 117575, Singapore.

<sup>2</sup>Department of Biomedical Engineering, National University of Singapore, Singapore 117583, Singapore.

<sup>3</sup>Department of Mechanical Engineering, National University of Singapore, Singapore 117575, Singapore.

\*Correspondence to: Chien Yi Wee, Department of Mechanical Engineering, National University of Singapore, Singapore 117575, Singapore. Email: [wee\\_chien\\_yi@u.nus.edu](mailto:wee_chien_yi@u.nus.edu)

Received: August 21, 2023; Accepted: October 17, 2023; Published Online: October 28, 2023

Citation: Lim QRT, Cheng XY and Wee CY. An Insight to the Various Applications of Hydroxyapatite. *Advanced Materials Science and Technology*, 2023;5(2):0520879. <https://doi.org/10.37155/2717-526X-0502-1>

**Abstract:** Hydroxyapatite is a naturally occurring calcium phosphate widely used in biomedical applications because of its osteoconductivity, biocompatibility and it possesses the closest chemical similarity to natural bone. Hydroxyapatite is also a versatile material and can be used in a plethora of ways beyond biomedical applications. This review summarises the applications of hydroxyapatite in biomedical, bioimaging, separation, purification, catalysis, surface treatment and energy storage applications. Finally, this review aims to shed light on its potential for new applications of hydroxyapatite in the future.

**Keywords:** Hydroxyapatite; Biomedical; Bioimaging; Purification; Catalysis; Coatings; Energy storage

## 1. Introduction

Hydroxyapatite (HAp) is a naturally occurring calcium phosphate widely used in biomedical applications because of its osteoconductivity, biocompatibility and it possesses the closest chemical similarity to natural bone. The chemical formula for pure HAp is  $\text{Ca}_{10}(\text{PO}_4)_6(\text{OH})_2$  and each molecule of HAp contains 5 pairs of positively-charged calcium ions, 2 phosphate triplets with 6 negatively-charged oxygen atoms each, and 2 hydroxyl residues. HAp has a theoretical composition of 39.68 wt% Ca, 18.45 wt% P with a Ca/P weight ratio of 2.151 and a

calcium-to-phosphate (Ca/P) molar ratio of 1.67. HAp crystals belong to the P63/m space group with lattice parameters  $a = b = 9.432 \text{ \AA}$ ,  $c = 6.881 \text{ \AA}$  and  $\gamma = 120^\circ$ . Pure HAp is white in colour while naturally occurring HAp may contain colourations depending on the mechanism and environment in which it was formed<sup>[1]</sup>.

HAp is typically synthesised via wet chemical precipitation due to its scalability and ease of operation. Other methods of producing hydroxyapatite include hydrothermal and solvothermal methods, solid-state reactions, electrochemical deposition, sol-gel methods, spray drying, biomimetic methods and microemulsions. HAp may also be synthesised using a combination of



the aforementioned methods, depending on the desired properties of the final HAp product<sup>[2,3]</sup>.

Aside from its biocompatibility, bioactivity and osteoconductivity, HAp also possesses high hardness, insolubility in water, excellent chemical and thermal stability, radiopacity, porosity control during synthesis and ion exchange properties<sup>[1]</sup>. HAp has been employed extensively in biomedical applications. Yet its intrinsic array of properties enable HAp to also be an attractive candidate for applications beyond the biomedical field. Hence, this review summarises the various applications of HAp, both in biomedical and non-biomedical fields. Different ways of how HAp is utilised for each application will be highlighted. Finally, this review aims to shed light on potential new applications of hydroxyapatite in the future.

## 2. Biomedical Applications

### 2.1 Bone Tissue Engineering

The primary aim of bone tissue engineering is to develop strategies to repair, regenerate, or replace damaged or lost bone tissues due to trauma, disease, or defects<sup>[4]</sup>. HAp is a versatile biomaterial in the field of bone tissue engineering. HAp is a natural component of bone, providing the inorganic mineral matrix that imparts its rigidity and strength<sup>[5]</sup>. Apart from its physiochemical properties, HAp has gained significant attention in bone tissue engineering due to its biochemical properties such as biocompatibility, osteoconductivity, and ability to bond with living bone<sup>[6]</sup>. HAp exhibits excellent biocompatibility, indicating that it can coexist with living tissues without triggering an adverse immune response or inflammation reaction<sup>[7]</sup>. Osteoconductive materials like HAp are essential for enabling the natural regeneration of bone tissue. HAp functions as a favourable substrate for bone cells to attach, proliferate, and migrate. Hence, this makes HAp applicable as a scaffold, guiding and supporting bone tissue growth in the defect area. The resemblance of HAp's chemical composition to the mineral phase of natural bone brings about good biocompatibility which facilitates seamless integration of HAp with surrounding native bone tissues, enhancing bone healing and bone tissue regeneration<sup>[8]</sup>. HAp is often combined with other biomaterials to become a composite scaffold system providing a three-dimensional framework with desired

mechanical properties for cellular organisation and growth<sup>[9]</sup>. Wee *et al.*<sup>[3]</sup> demonstrated that HAp can be used as a microsphere scaffold. The rough surface morphology of HAp aids in cell attachment, creating an environment favourable for further cell proliferation and differentiation. Bernardo *et al.*<sup>[10]</sup> developed 3D printed composite scaffolds of polylactic acid (PLA) and HAp using fused deposition modelling (FDM) with the intent of having a tailored scaffold morphology and high precision shape to match the defect site. These PLA/HAp scaffolds displayed good osteogenic differentiation without osteogenic stimuli. HAp has a slow rate of resorption, allowing it to maintain its structural integrity for long periods of time<sup>[11]</sup>. This is crucial if HAp is to be used as a synthetic bone graft. The slow rate of resorption allows the bone graft to provide long-term support during bone healing phase, whereby the bone graft is slowly replaced by newly formed bone. The resorption rates of HAp scaffolds can be modified and fine-tuned by incorporating trace elements into the HAp matrix through ionic substitution<sup>[10]</sup>. Shuai *et al.*<sup>[11]</sup> developed a composite scaffold through 3D laser printing encompassing HAp into poly-L-lactic acid (PLLA) and polyglycolic acid (PGA) to tune the degradability of the scaffold. The degradability of the scaffold matrix as a result of the polymeric PGA and PLLA components induced pore formation and exposed the HAp in the scaffold matrix. New bone formation and blood vessel formation was seen to bridge defect sites after 8 weeks of implantation in rabbit models. HAp is also used as bone fillers to fill in gaps in bone defects and damaged bone to facilitate good integration with the host tissue, promoting effective bone tissue regeneration<sup>[12]</sup>. For larger bone defects which require mechanical support such as metallic implants used in hip prosthesis or joint replacements, the mechanical properties of the implant must be robust. HAp alone cannot be used alone due to its brittle nature<sup>[13]</sup>. In such cases, HAp is employed as surface coatings on metallic implants. The rough surface morphology and bioactive properties of HAp coatings improve the overall implants' integration to surrounding bone tissues, reducing the risk of implant non-union which may result in implant failure. Ripamonti *et al.*<sup>[14]</sup> uniformly coated titanium grade implants with hydroxyapatite displayed induced bone formation indicating the favourability of HAp in

promoting bone regeneration.

## 2.2 Dental Applications

Similar to applications in bone tissue engineering, HAp finds numerous applications in dentistry due to its biocompatibility, bioactivity, and similarity to the mineral component of teeth<sup>[15]</sup>. It has become an essential biomaterial for various dental applications, including tooth restoration, dental implants, and preventive treatments. HAp can be used as a dental filling material to repair cavities caused by tooth decay<sup>[16]</sup>. HAp-based dental fillings have the advantage of being biocompatible and having a similar chemical composition to natural tooth enamel. This facilitates better integration with the tooth structure, reducing the risk of secondary decay and improving the longevity of the tooth restoration. Akhtar *et al.*<sup>[17]</sup> showed that cubic-shaped nano-hydroxyapatite (n-HAp) particles displayed good hardness and enhanced anti-wear properties which is important for dental fillings. Dental implants are artificial tooth roots that are surgically placed into the jawbone to support dental prostheses like crowns, bridges, or dentures. HAp-coated dental implants enhance osseointegration, which is the process of implant fusion with the surrounding bone, promoting a more stable and long-lasting restoration<sup>[18]</sup>. Ansari *et al.*<sup>[19]</sup> explored the use of polycaprolactone/fluoride substituted hydroxyapatite (PCL/FHA) nanocomposite coatings for potential application as tooth implant coating. They showed that the coatings can be deposited homogeneously onto the substrate of interest with no cracks. It also displayed a good degree of corrosion resistance with desired properties for surface roughness and cell adhesion. In dental procedures such as ridge augmentation or sinus lifts, where there is insufficient bone volume for dental implant placement, hydroxyapatite can be used as a bone graft material<sup>[20]</sup>. HAp-based bone grafts support bone regeneration and provide a scaffold for new bone formation, facilitating successful implant placement. HAp is also used as a re-mineralizing agent to combat early stages of tooth decay<sup>[21]</sup>. Multiple research studies showed the benefits of nano-HAp when used in toothpaste and mouthwash formulations to aid repair and strengthen tooth enamel, potentially reducing tooth sensitivity and preventing dental caries, reducing the likelihood of severe dental caries, avoiding invasive treatment<sup>[22-24]</sup>.

## 2.3 Hydroxyapatite-Based Drug Delivery Systems

Apart from being ideal candidates for bone and dental implants, the application of HAp can be seen in drug delivery systems due to its unique properties such as its biocompatibility with the physiological environment, ability to adsorb drugs, and tunable controlled release properties<sup>[25]</sup>. They can be utilised to deliver therapeutic drugs or molecules to specific target sites in a controlled and sustained manner. This can be done through surface functionalization of HAp with ligands and biomolecules such as peptides or antibodies to identify specific receptors on target tissues or cells<sup>[26]</sup>. The porous morphological structure of HAp facilitates high drug-loading capacity. HAp nanoparticles have demonstrated their effectiveness in adsorbing or encapsulating therapeutic drugs which includes anticancer agents, antibiotics, and growth factors<sup>[27]</sup>. The slow degradation rate of HAp enables the gradual controlled and sustained release of drugs over an intended period. As HAp can be substituted with different types of ions, its degradation rate can be further fine-tuned to match the required duration for the therapeutic drug release application<sup>[28]</sup>. Kong *et al.*<sup>[29]</sup> developed a composite system of HAp with hyaluronic acid (HA) and polyethyleneimine (PEI). Doxorubicin (DOX), a cancer drug was loaded and displayed a pH responsive release profile. The targeting property of this composite system shows high favorability to CD44 receptors on cancer cells. Sustained release of DOX from the HAp-PEI-HA system displayed a high therapeutic effect. In addition to specific drug delivery and controlled drug release, HAp is also used for bone targeted therapy. The natural affinity of HAp for bone tissue makes it an ideal biomaterial for bone related drug delivery. Treatment of bone related diseases such as bone metastases and osteoporosis can be done by delivering therapeutic agents to the specific bone tissue site<sup>[30]</sup>. Maia *et al.*<sup>[31]</sup> demonstrated the use of radio labelled hydroxyapatite nanoparticles with technetium showed good stability and high affinity for bone tissues, increasing bone uptake over time, indicating its potential application for bone related diseases. Furthermore, HAp has the potential to be utilised in regenerative medicine. Growth factors and biomolecules can be encapsulated in HAp carriers or microspheres to stimulate cell proliferation and tissue repair, promoting tissue regeneration<sup>[32-34]</sup>.

## 2.4 Hydroxyapatite-Based Fluorescent Probes

Aside from bone and dental implants, drug delivery systems, HAp are increasingly popular in the bioimaging field. HAp-based fluorescent probes are a class of nanomaterials that combine the unique properties of HAp with the ability to emit fluorescent signals<sup>[35]</sup>. As a result, these probes have garnered significant attention in biomedical research and applications due to their biocompatibility, tunable fluorescence properties, and potential for various imaging and sensing applications. Synthesising HAp-based fluorescent probes involves incorporating fluorescent molecules or quantum dots into the HA structure<sup>[36]</sup>. These probes have the characteristic ability to emit light at specific wavelengths upon excitation, facilitating sensitive and selective detection in imaging and sensing applications. Apart from its light emitting capabilities, HAp-based fluorescent probes can be engineered with pH-sensitive characteristics<sup>[37]</sup>. In this case, the fluorescence intensity and emission wavelengths can be changed when the pH of the environment changes. This is useful when these probes come into the physiological system when they interact with cellular or tissue environments. Additionally, these HAp-based probes can be modified to selectively bind to cells or tissues of interest. This can be done by functionalizing these probes with biomolecules and ligands which have the traits of recognizing specific cell receptors to achieve specific targeted imaging<sup>[38]</sup>. HAp-probes can also be applied in intracellular imaging applications. HAp-probes may be internalised by cells and monitor ongoing processes and responses taking place in cells<sup>[39]</sup>. The fluorescence characteristic of the probes can be used to track real-time drug delivery and drug release profile<sup>[40]</sup>. This application is valuable in data collection and allows researchers to have a better understanding of the drug's efficacy and pharmacokinetics. Applications of such HAp-probes can be seen in bone imaging due to HAp's natural affinity for bone tissue. This enables close monitoring of bone regeneration processes and scaffold implants over time.

## 2.5 Hydroxyapatite in Near-Infrared Imaging

Near-infrared imaging (NIR) is a non-invasive imaging technique used to visualise biological tissues and structures with high spatial resolution<sup>[41]</sup>. As the name suggests "near-infrared", this technique utilises light

in the near-infrared spectrum (700 nm to 900 nm) for tissue visualisation. As HAp has excellent light scattering and absorption properties in the near-infrared range, this makes HAp a good optical material to function as a contrast agent in NIR imaging<sup>[42]</sup>. Under NIR wavelength, images of tissue structures can be visually enhanced when subjected to *in-vitro* or *in-vivo* imaging. It is also worth pointing out that such light at the near-infrared wavelength allows deeper tissue penetration with reduced amounts of background autofluorescence. Similar to biomedical applications of HAp, HAp NIR imaging agents can be modified for specific monitoring applications<sup>[43]</sup>. This is usually done by functionalizing HAp NIR imaging agents with targeting ligands to ensure that site-specific imaging is achieved for more accurate diagnosis and monitoring. HAp NIR imaging is most commonly applied for bone imaging. As HAp is a natural inorganic component of natural bone, the incorporation of NIR fluorescent dyes into HAp nanoparticles facilitates the development of bone targeted imaging agents<sup>[44]</sup>. These agents can be utilised for diagnosing bone diseases and monitoring bone related processes. Due to the non-invasive nature of this technique, HAp NIR imaging agents can also be employed to monitor bone tissue growth and progress of bone scaffold integration post implantation. This will aid researchers in assessing the effectiveness of bone tissue engineering scaffolds. HAp NIR imaging agents may also function as carriers for drug applications<sup>[45]</sup>. Incorporation of imaging agents and therapeutic molecules into HAp nanoparticles, monitoring of real-time drug release and drug distribution profile can be achieved. This application is beneficial for optimising treatment methods.

## 2.6 Hydroxyapatite for Theranostics

Theranostics is an emerging field that combines therapeutic and diagnostic functions in a single platform<sup>[46]</sup>. The main aim of theranostics is to develop personalised medicine approaches by integrating diagnostic imaging and targeted therapy to improve treatment outcomes. HAp-based theranostic agents have gained considerable attention due to their biocompatibility, versatility, and ability to serve as a platform for both imaging and therapeutic components. By integrating diagnostic imaging and therapeutic functionalities, HAp-based theranostics offer a multifaceted approach to medical treatments.



The ability to monitor treatment response in real-time allows for early adjustments to therapy and personalised treatment plans. HAp is seen in many different imaging modalities such as computed tomography (CT), near-infrared imaging (NIR) and magnetic resonance imaging (MRI) for more accurate visualisation of tissue structures<sup>[47]</sup>. Another application of HAp in theranostics is seen in drug delivery applications. HAp nanoparticles can encapsulate therapeutic drug molecules, delivering them to the specific tissue of interest<sup>[48]</sup>. The release of therapeutic agents can be controlled to enable sustained and targeted delivery. Similar to the application of HAp in the earlier segments, HAp theranostic agents can be functionalized with ligands or biomolecules to enable them to selectively bind to cells or tissues of interest<sup>[49]</sup>. Such an approach would mean better efficiency and specificity of a therapy or treatment, reducing the likelihood of side effects or overdose. HAp theranostic agents can be applied to the oncology field. HAp nanoparticles can be engineered to deliver chemotherapy drugs or gene therapies to tumour cells while being visualised using imaging modalities for accurate tumour targeting and therapy monitoring<sup>[50]</sup>. HAp theranostics can also be used in tissue engineering and regenerative medicine applications<sup>[51]</sup>. HAp scaffolds can be functionalized with growth factors or drugs to promote tissue regeneration, while the imaging capabilities of HA enable non-invasive monitoring of

tissue growth and scaffold integration.

### 3. Separation and Purification Applications

#### 3.1 Protein and Virus Separation

HAp contains positively-charged calcium ions (C-sites) and negatively-charged phosphate groups (P-sites). The symmetry of the P63/m space group distributes the C-sites and P-sites regularly throughout the HAp crystal structure. Positively charged and negatively charged groups on biomolecules experience electrostatic attraction with P-sites and C-sites of HAp respectively. Similarly, positively charged and negatively charged groups on biomolecules will experience electrostatic repulsion with C-sites and P-sites on HAp respectively. Metal affinity interactions also occur between C-sites on HAp and charged species of biomolecules, and are much stronger than regular electrostatic interactions. The interactions between HAp and proteins during separation and purification applications are illustrated in **Figure 1**. The extent of interaction between biomolecules and HAp depends on the abundance and structures of functional groups present on the biomolecules. In essence, different biomolecules experience a different extent of interactions and hence different binding capacity with HAp. The difference in interactions with different biomolecules enable HAp to be deployed as a material for separation and purification of biological compounds and biomolecules in chromatography applications<sup>[52]</sup>.

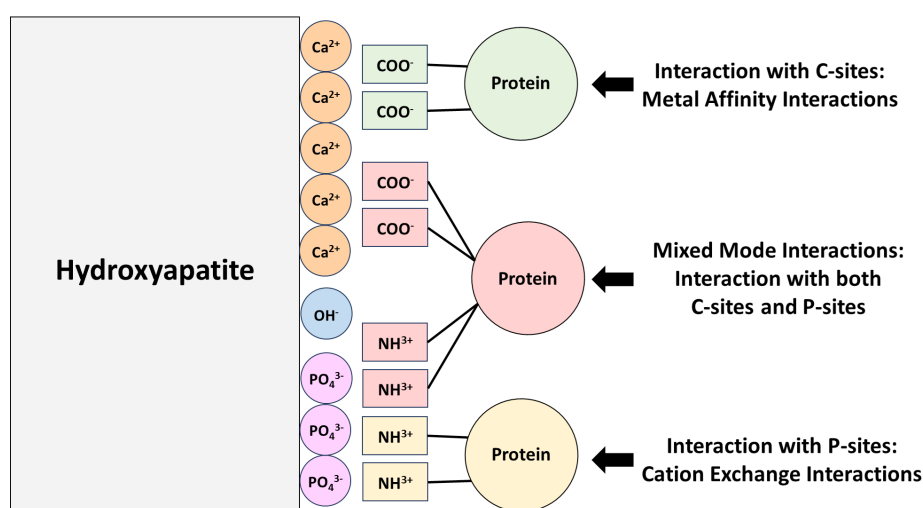


**Figure 1.** Schematic diagram of the different interactions between hydroxyapatite and proteins for separation applications

HAp is frequently used as chromatography media for the purification of proteins. Recent advances in

HAp chromatography include protein separation using naturally-derived HAp<sup>[53]</sup> and HAp nanoparticles<sup>[54]</sup>.

HAp chromatography has gained popularity over the years because of its exceptional performances in protein separation and purification. Jing *et al.*<sup>[55]</sup> employed HAp chromatography media to purify and analyse histones (H2B) in their study on site-specifically succinylated histone at K77 residue influences the structure and dynamics of nucleosomes. Proteins purified via HAp chromatography also include bone morphogenetic protein<sup>[56]</sup>, albumin<sup>[57,58]</sup>, antibodies<sup>[59,60]</sup>, and enzymes<sup>[61]</sup>. Wang and Carta<sup>[59]</sup> investigated the influence of HAp pore size on protein adsorption and adsorption kinetics using monoclonal antibody (mAb) monomer-dimer mixtures. In Wang and Carta's study, two types of HAp with pore sizes 30 nm and 49 nm were chosen, and the phosphate buffers used were at pH 7, which is below the isoelectric point of mAb and prevents anion exchange from occurring between mAb and the HAp surface. Adsorption of mAb monomers onto the surface of HAp occurs via electrostatic interactions and is controlled by cation exchange. The adsorption kinetics of mAb onto HAp is controlled by pore diffusion and the HAp with a smaller pore size had a higher mAb binding capacity but slower adsorption kinetics.

The ability of HAp to separate proteins endows them the ability to separate viruses as well. Viruses contain a protein coat called a capsid, regardless of structure. The proteins in the capsid can interact and be separated in HAp chromatography like non-viral proteins<sup>[62]</sup>. Tomato bushy stunt virus (TBSV) was purified by Tleukulova *et al.*<sup>[63]</sup> using HAp chromatography. TBSV viral particles did not adsorb onto HAp at low concentrations of sodium phosphate buffer and flowed through the column instead. Meanwhile, the proteins extracted from plants infected by TBSV adsorbed onto the HAp sorbent. HAp chromatography was used for the purification of poliovirus by Kurosawa *et al.*<sup>[64]</sup> They separated poliovirus Sabin type 2, dengue virus (DENV) type 1 and influenza virus with HAp chromatography. Lin *et al.*<sup>[65]</sup> separated DENV defective interfering particles (DENV-DIP) using HAp chromatography to evaluate the antiviral activity of DENV-DIP. HAp acted as both the matrix and the ligand during the DENV-DIP purification chromatography process.

### 3.2 Enzyme Purification and Immobilisation

Enzymes are proteins that act as biological catalysts to accelerate metabolism and chemical reactions in

the human body. HAp nanoparticles are used for enzyme purification and immobilisation due to their high surface-area-to-volume ratio and protein affinity. Spherical and flower-shaped HAp nanoparticles were recently produced by Lin *et al.*<sup>[58]</sup> for the immobilisation of albumin. Flower-shaped HAp nanoparticles had a superior adsorption-extraction ability for albumin compared to spherical HAp nanoparticles. Flower-shaped HAp nanoparticles are able to adsorb albumin within a short period of time after being exposed to serum albumin. The simplicity and rapidness of albumin immobilisation onto flower-shaped HAp nanoparticles displays great potential for employing HAp in cancer screening applications<sup>[58]</sup>. Magnetic HAp (MHAp), iron(III) oxide and reduced graphene oxide (rGO) composites (MHAp/rGO) were synthesised by Bharath *et al.*<sup>[66]</sup> for selective separation of haemoglobin (Hb). The MHAp/rGO composite had a maximum adsorption capacity of 1012 mg/g at near the isoelectric point of Hb, highlighting the immense potential of HAp composites in protein separation and immobilisation for diagnostics.

HAp and HAp composites also see use in enzyme immobilisation and storage. HAp and zirconium oxide composites (HAp-ZrO<sub>2</sub>) were investigated by Almulaiky *et al.*<sup>[67]</sup> for their ability to immobilise and store  $\alpha$ -amylase. HAp-ZrO<sub>2</sub> composites had better immobilisation ability of  $\alpha$ -amylase than HAp.  $\alpha$ -amylase also exhibited enhanced storage stability and catalytic activity when immobilised onto HAp-ZrO<sub>2</sub> compared to HAp. Nickel and copper modified HAp nanoparticles successfully immobilised xylanase enzymes and shows immense promise for the development of recyclable industrial biocatalysts in a study conducted by Coutinho *et al.*<sup>[68]</sup>. Coutinho *et al.*<sup>[69]</sup> also developed HAp and cobalt ferrite (CoFe<sub>2</sub>O<sub>4</sub>) composites that support a wide range of enzyme immobilisation including the immobilisation of xylanase, phytase and  $\beta$ -glucosidase. The immobilised enzymes could be separated from the HAp-CoFe<sub>2</sub>O<sub>4</sub> composites by an external magnetic field or centrifugation, and had displayed good recyclability. Interestingly, HAp was utilised in chromatography for the purification of enzymes in plants. Yamasawa *et al.*<sup>[70]</sup> purified D-cysteine desulhydrase (D-CDes) from rice seed (*Oryza sativa L.*) via a 4-step chromatography procedure involving HAp chromatography. Holková

*et al.*<sup>[71]</sup> purified lipoxygenases (LOX) from opium poppy cultures (*Papaver somniferum L.*) via a two-step chromatography process. LOX underwent ammonium sulfate precipitation before chromatography with HAp sorbent to be purified from *Papaver somniferum L.*. Rohman *et al.*<sup>[72]</sup> purified catalase from the leaves of barley (*Hordeum vulgare L.*) to examine the role of catalase in *Hordeum vulgare L.* under saline stress. Proteins from the leaves of *Hordeum vulgare L.* were extracted in Tris-HCl buffer before a 3-step chromatography process involving HAp chromatography to obtain catalase.

### 3.3 Solid Phase Microextraction

The excellent performance of HAp in chromatography and separation techniques makes it an attractive material in solid phase microextraction (SPME) and solid phase extraction (SPE). SPME is an equilibrium extraction technique that separates analytes from a complex medium using a solid stationary phase. SPME is solvent-free and easy to automate, with reusable solid phases and low cost<sup>[73]</sup>. SPE is a solid-liquid extraction technique which uses the solid phase to remove impurities from the target analyte dissolved in the liquid phase. SPE has the advantages of high reproducibility, speed and versatility while requiring minimal solvent usage as a cost-effective separation technique<sup>[74]</sup>. Wang *et al.*<sup>[75]</sup> built a HAp surface-functionalized monolithic column of polydopamine (PDA) and urea-formaldehyde resin (UF) for the SPME and high performance liquid chromatography (HPLC) of zoleronic acid (ZOD) and risedronic acid (RID) in serum. The HAp/PDA/UF monolithic column exhibited excellent selectivity during ZOD and RID extraction due to its calcium-phosphate anion exchange interactions. Wang *et al.*<sup>[76]</sup> also built HAp/UF monolithic columns for selective extraction of adenosine triphosphate (ATP) and phosphorylated metabolites of ATP using SPE. This HAp/UF monolithic column had a large surface area and displayed desirable extraction selectivity and efficiency for ATP and phosphorylated metabolites of ATP. Rahmani *et al.*<sup>[77]</sup> fabricated a monolithic array of TiO<sub>2</sub>/HAp nanowires for SPME of DOX from water and human urine. The hollow fibre geometry of the TiO<sub>2</sub>/HAp monolithic array allowed for high throughput SPME. The TiO<sub>2</sub>/HAp hollow fibres had a negative surface charge at acidic pH, which binds positively charged DOX via electrostatic interactions. SPME using the TiO<sub>2</sub>/HAp monolithic

array did not require sample preparation and did not have a significant matrix effect. Aside from monolithic columns, HAp can be used directly as the solid phase in SPE. Rahmipoor *et al.*<sup>[78]</sup> packed HAp nanoparticles into a needle trap device (NTD) for the extraction of phenolic compounds from air. HAp nanoparticles in the NTD had a high adsorption capacity for phenol, 2-chlorophenol, o-cresol, and p-cresol. The limit of quantification (LOQ) and limit of detection (LOD) of phenol, 2-chlorophenol, o-cresol, and p-cresol were 0.004-0.023 ng/mL and 0.001-0.01 ng/mL respectively. Bayatloo *et al.*<sup>[79]</sup> synthesised MHAp using iron(III) oxide and HAp to fabricate a magnetic adsorbent of  $\beta$ -cyclodextrin ( $\beta$ -CD) and MHAp. The MHAp/ $\beta$ -CD adsorbent was utilised for extraction of bisphenol A (BPA) from human urine samples, bottled water and baby bottle samples via magnetic SPE. BPA adsorbs onto MHAp/ $\beta$ -CD through hydrophilic interactions and forming host-guest inclusion complexes. MHAp/ $\beta$ -CD adsorbent had a LOD of 0.06 ng/mL and LOQ of 0.18 ng/mL for BPA, along with good reproducibility and repeatability.

## 4. Catalysis and Environmental Applications

### 4.1 Water Purification

HAp is porous and has a large surface area, giving it a high adsorption capacity for target substances. The synthesis of HAp controls the porosity and surface properties of the final HAp product, which in turn controls the particle size selectivity, antifouling properties and surface properties of HAp. HAp also has excellent regenerability, making it a cost-effective filtration medium in repetitive or continuous purification processes. These properties, along with hardness and chemical stability, make HAp a favourable candidate for environmental applications. The key properties for HAp in environmental applications are its low toxicity, regenerability, heavy metal affinity, ion exchange capacity and adsorption capabilities. The ion exchange capabilities of HAp confer it a high capacity for the capture and removal of divalent heavy metal ions from wastewater<sup>[80-82]</sup>. Xiong *et al.*<sup>[83]</sup> fabricated a biomimetic aerogel using HAp nanowires (HApNW) and chitosan for water purification. HApNWs were the carriers for catalyst nanoparticles and underwent structure-function integration with chitosan to produce biomimetic aerogels. HApNW-chitosan biomimetic aerogels had an interconnected cellular structure, unidirectional aligned

channels, nanowire-interwoven networked pore wall, and evenly distributed catalyst nanoparticles, which allowed it to display a permeability of  $1786 \text{ L/m}^2 \cdot \text{h}$ , 97.6% treatment efficiency and outstanding stability and recyclability under continuous flow catalytic degradation of methylene blue (MB). The HApNW-chitosan aerogel displayed an efficiency of 86.7% for solar energy-driven seawater desalination and wastewater purification under one sun irradiation, and excellent antifouling and antibacterial properties. Zhang *et al.*<sup>[84]</sup> fabricated a filter paper using cellulose fibres (CF) and HApNW for water purification. The HApNW/CF filter paper displayed a removal of  $\text{TiO}_2$  nanoparticles greater than 98.61% and up to 100% removal of bacteria in water via size exclusion. The HApNW/CF filter paper also had adsorption capacities of 508.16 mg/g and 273.97 mg/g for lead(II) ions and methyl blue respectively.

Pollutants are removed from wastewater by adsorption due to surface interactions or ion exchange with Hap<sup>[85]</sup>. Jung *et al.*<sup>[86]</sup> fabricated HAp/biochar (BC) nanocomposites for the removal of copper(II) ions from aqueous media. Ion exchange between copper(II) ions in aqueous media and calcium ions on the surface of HAp/BC nanocomposites, as well as the formation of inner sphere complexes on the surface of the HAp/BC nanocomposites appeared to be the mechanism for copper(II) ion removal. The mechanism of ion exchange between copper(II) ions and calcium ions in HAp is shown in **Figure 2**. The overall adsorption

rate of copper(II) ions onto HAp/BC is controlled by film diffusion as the dominant mechanism, with interparticle diffusion being the secondary mechanism. The adsorption of copper(II) ions onto HAp/BC adsorption process followed the pseudo-second-order model with the maximum adsorption capacity of 99.01 mg/g at 298 K<sup>[86,87]</sup>. Wang *et al.*<sup>[88]</sup> prepared HAp microspheres for the removal of coomassie brilliant blue (CBB) from wastewater. Adsorption of CBB onto HAp microspheres was found to be an endothermic and spontaneous process, with HAp microspheres having a maximum adsorption capacity of 83.8169 mg/g for CBB. HAp microspheres also had good recyclability, with its adsorption capacity for CBB decreasing to 82.59%, 72.67% and 58.39% after the first, second and third regeneration cycles respectively. Azeez *et al.*<sup>[89]</sup> doped HAp with silver nanoparticles (AgNPs) for the removal of congo red (CR) and MB. The AgNP-doped HAp had an isoelectric point (pI) of 7.09 and exhibited maximum adsorption of CR and MB at pH 2 and pH 11 respectively. AgNP-doped HAp had monolayer adsorption capacities of 1039.07 mg/g to 205.49 mg/g for MB and 47.75 mg/g to 159.11 mg/g CR from 303 K to 313 K. The adsorption of CR and MB onto AgNP-doped HAp followed pseudo-second order kinetics and along with intramolecular diffusion, controlled the rate-determining step of the process. The adsorption of MB and CR onto AgNP-doped HAp was spontaneous but exothermic due to the overall decrease in entropy.

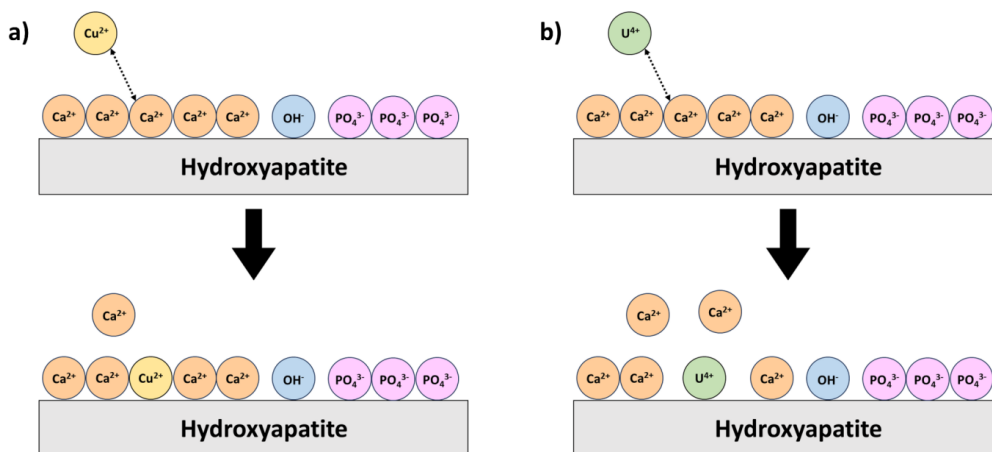


**Figure 2.** A schematic diagram of ion exchange between calcium ions in hydroxyapatite and (a) divalent metal ions and (b) tetravalent metal ions. Copper(II) and uranium(IV) ions are used as examples to illustrate the ion exchange mechanism

HAp is not used as a material for the removal of phosphates during water purification. Instead, the wet precipitation of HAp is exploited for the removal of

phosphates from water. HAp is the most insoluble calcium phosphate and readily precipitates in water the moment it is formed. The simplest method of water



purification is the addition of calcium hydroxide to remove phosphates via precipitation of hydroxyapatite. Chang *et al.*<sup>[90]</sup> used a phosphate crystallisation-filtration process (PCF) to immobilise phosphate in wastewater via crystallisation of HAp. Calcium ions were added to wastewater under controlled pH in a PCF reactor and the resulting HAp crystals were precipitated and crystallised on the surface of calcite particles. This PCF process had a removal efficiency of 90.0%, 86.5% and 79.7% for total phosphorus (T-P), orthophosphate as phosphorus ( $\text{PO}_4\text{-P}$ ), and suspended solids (SS) respectively. Effluent SS and T-P contents were less than 10 mg/L and 0.2 mg/L respectively, from the PCF process. The development of different filter media which can release calcium ions into water also enable the precipitation of HAp. An alternating anaerobic/aerobic biofilter (A/OBF) reactor constructed by Sun *et al.*<sup>[91]</sup> was able to successfully enrich phosphorus accumulating organisms (PAOs). Phosphate removal achieved via consumption by PAOs and HAp crystallisation on the biofilms generated in the A/OBF reactor. HAp was used by Bao *et al.*<sup>[92]</sup> for phosphate recovery from iron(III) oxide/carbon filter media (FCM) in a biological aerated filter (BAF). Phosphate recovery was achieved by the reaction of calcium ions, phosphate ions and hydroxide ions to form and precipitate HAp on the FCM. In the studies conducted by Sun *et al.*<sup>[91]</sup> and Bao *et al.*<sup>[92]</sup> the filter media acted as a reservoir for calcium ions that prevents them from being released until the filter media is used for its intended water purification purposes. Phosphates in wastewater will react with the high concentration of calcium ions released from the filter media in aqueous environments, readily forming and precipitating as HAp crystals. HAp has low solubility in water and thus will not readily dissociate in aqueous media<sup>[93]</sup>.

#### 4.2 Removal of Toxic Emissions

HAp has been shown to be a vital material for

effectively removing nitrous oxides from emissions. Thermal stability, high ion exchange capabilities and adsorption capacity enable HAp to be easily doped with other metals (see **Figure 3**) Doped HAp has the ability to act as a catalyst for the conversion of nitrous oxides to non-toxic gases. Copper-doped HAp (Cu-HAp) catalysts fabricated by Tounsi *et al.*<sup>[94]</sup> exhibited excellent catalytic properties, with a 20% and 85% conversion of nitric oxide (NO) to ammonia at 100 °C and 350 °C respectively. Silver-doped HAp (Ag-HAp) catalysts prepared by Kumar *et al.*<sup>[95]</sup> displayed exceptional performance in the conversion of nitrogen oxides ( $\text{NO}_x$ ) to nitrogen. Ag-HAp with 1.5 wt% Ag attained the highest conversion of  $\text{NO}_x$  to nitrogen of 70% at 375 °C. Recently, Wei *et al.*<sup>[96]</sup> developed cobalt-doped HAp (Co-HAp) catalysts using cobalt(II,III) oxide ( $\text{Co}_3\text{O}_4$ ) impregnated onto synthetic HAp (HAp-syn) and natural HAp (HAp-n). Both Co-HAp-syn and Co-HAp-n catalysts displayed superior catalytic activity for the decomposition of nitrous oxide ( $\text{N}_2\text{O}$ ) compared to a pure  $\text{Co}_3\text{O}_4$  catalyst. The  $\text{N}_2\text{O}$  decomposition reaction follows first-order reaction kinetics. Furthermore, Co-HAp-n catalysts display higher catalytic activity than their counterparts fabricated using synthetic HAp. Natural HAp was shown to facilitate the reduction of cobalt(III) to cobalt(II) during the  $\text{N}_2\text{O}$  decomposition. The onset of  $\text{N}_2\text{O}$  decomposition begins at 300 °C and the reaction is completed at 460 °C in the presence of Co-HAp-n catalysts. Meanwhile, Co-HAp-syn catalysts catalyse  $\text{N}_2\text{O}$  decomposition between 340 °C to 540 °C. However, the catalytic activity of Co-HAp-syn is inhibited by oxygen or water. This inhibition of catalytic activity by oxygen or water is not observed for Co-HAp-n. Co-HAp-n also displays greater catalytic activity than Co-HAp-syn in the presence of oxygen, carbon dioxide and  $\text{NO}$ <sup>[96]</sup>.

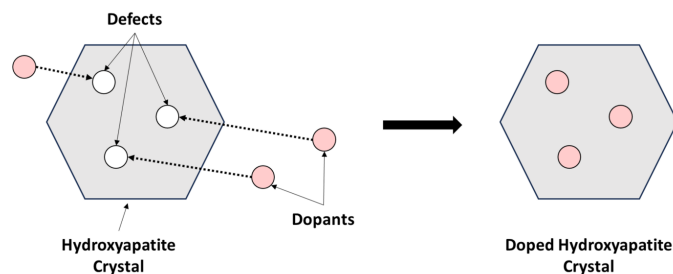


**Figure 3.** Schematic diagram illustrating hydroxyapatite doping

HAp can also act as a support for metal nanocatalysts, which are usually rare and expensive metals. The regenerability of HAp allows for easy recyclability of metal nanocatalysts that have been doped onto HAp. In a study conducted by Shokouhimehr *et al.*<sup>[97]</sup>, HAp-supported palladium (HAp-sPd) catalysts were synthesised for the catalytic reduction of nitroarenes in water and for the environmentally friendly oxidation of alcohols. The HAp-sPd catalysts exhibited a high catalytic efficiency, selectivity, and yield for the reduction of nitroarenes with aqueous sodium borohydride (NaBH<sub>4</sub>) and for the oxidation of alcohols with hydrogen peroxide (H<sub>2</sub>O<sub>2</sub>). The HAp-sPd catalysts possess good recyclability, being able to produce a yield of above 85% for both the reduction of nitroarenes and oxidation of alcohols after being separated and regenerated from the reaction products 6 times. Bahadorikhalili *et al.*<sup>[98]</sup> fabricated thiourea functionalized magnetic HAp (SUMHAp) as supports for AgNPs. The SUMHAp/AgNP catalysts displayed remarkable catalytic activity in the reduction of primary amines and the selective oxidation of 4-nitrophenol (4NP). Pristine SUMHAp/AgNP catalysts had a similar adsorption-desorption isotherm as SUMPHAp/AgNP catalysts that have undergone 10 cycles of regeneration, which is a testament to the excellent recyclability of SUMHAp/AgNP. Layek *et al.*<sup>[99]</sup> synthesised HAp-supported gold (HAp-sAu) catalysts for the degradation of azo dyes and reduction of nitroarenes. The HAp-sAu catalysts were fabricated via a deposition-precipitation process using gold(III) chloride trihydrate solution with a HAp support. The HAp-sAu catalysts displayed an excellent catalytic effect with the rapid reduction of 4-nitrophenol and degradation of CR and methyl orange (MO) dyes. This HAp-sAu catalyst could be recovered via centrifugation and maintained desirable catalytic activity after five cycles of regeneration.

### 4.3 Nuclear Waste Management

The ease of doping and ion exchange ability of HAp makes it a viable material for the management of nuclear waste. Radioactive corrosion products chromium, cobalt, copper, zinc, manganese, iron, and nickel can be readily adsorbed and immobilised by HAp. HAp used in nuclear waste management does not require additives, chemical treatment or complex equipment, yet it is an eco-friendly process with no harmful effects on the environment<sup>[100]</sup>. A MHAp

composite made from iron(III) oxide and HAp was used in conjunction with a cold-sintering technique by Venkatesan *et al.*<sup>[101]</sup> to remove radioactive ionic corrosion products from nuclear reactor coolant. The combination of MHAp and cold-sintering technique displayed a normalised leaching rate of 10<sup>-6</sup> g/m<sup>2</sup> · day to 10<sup>-7</sup> g/m<sup>2</sup> · day for all ions adsorbed, which is indicative of its ability to adsorb and immobilise radioactive ions in nuclear waste. MHAp has excellent adsorption properties that make it popular for removing radioactive heavy metal ions. Lu *et al.*<sup>[102]</sup> fabricated hexamethylene diamine tetramethylene phosphonic acid (HDTMP)-doped MHAp for the immobilisation of radioactive cobalt(II) and strontium ions. HDTMP-MHAp containing organic phosphine at a molar ratio of 10% to total phosphorus (10HDTMP-MHAp) was also fabricated in this study. HDTMP-MHAp had an adsorption capacity of 28.4 mg/g for cobalt(II) ions and 54.9 mg/g for strontium ions. Meanwhile 10HDTMP-MHAp had adsorption capacities of 172.3 mg/g and 320.7 mg/g for cobalt(II) ions and strontium ions respectively. Strontium and cobalt(II) ions irreversibly adsorb onto HDTMP-MHAp and will not desorb back into the aqueous system they originally came in<sup>[102]</sup>. MHAp/chitosan composites were produced by Le *et al.*<sup>[103]</sup> for the immobilisation of radioactive nickel(II) ions in aqueous media. MHAp/chitosan composites had a maximum adsorption capacity of 112.36 mg/g for nickel(II) ions, with the adsorption of nickel(II) onto MHAp/chitosan composites following pseudo-second order kinetics. The MHAp/chitosan composites had outstanding recyclability, being able to achieve an 85% efficiency for the immobilisation of nickel(II) ions after five regeneration cycles. High surface area HAp was also recently prepared by Kim *et al.*<sup>[104]</sup> for the removal of strontium radionuclides from water. High surface area HAp was also recently prepared by Kim *et al.*<sup>[104]</sup> for the removal of strontium radionuclides from water. The synthesised high surface area HAp attained a surface area up to 177.00 m<sup>2</sup>/g and a maximum adsorption capacity for strontium of 28.51 mg/g, proving to be a promising method for the removal of strontium radionuclides. Yang *et al.*<sup>[105]</sup> developed a HAp-perovskite composite for the immobilisation of iodine and cesium in radioactive waste. The HAp-perovskite composite displayed excellent chemical stability and desirable performance in the capture of

cesium and iodine.

The ability for doped HAp to capture uranium in radioactive waste spearheaded recent developments in nuclear waste management. The uranium capture capabilities of HAp is attributed to its excellent ion exchange capabilities. Recent literature has shown that doped-HAp is a promising candidate for the removal of uranium from wastewater. A study by Skwarek *et al.*<sup>[106]</sup> demonstrated that Ag-HAp adsorbs uranium via chemisorption, with a maximum adsorption capacity of 7.2 mmol/g. The mechanism of chemisorption is shown in **Figure 4a**. Zhou *et al.*<sup>[107]</sup> synthesised aluminium-doped HAp (Al-HAp) that efficiently immobilised uranium through the formation of complexes between uranium and the hydroxyl groups on the surface of HAp. Similarly, Szenknect *et al.*<sup>[108]</sup> demonstrated that surface complexation (see **Figure 4b**) and crystallisation was also responsible for the adsorption of uranium onto copper-doped HAp (Cu-HAp). Cu-HAp was able to be separated and regenerated from the complex for further uranium capture. MHAp has also been proven to be an efficient tool for uranium capture. El-Maghrabi *et al.*<sup>[87]</sup> prepared MHAp using HAp and iron(III) nitrate that had a total adsorption capacity of 310 mg/g for uranium, with adsorption following a pseudo second order reaction mechanism. Ou *et al.*<sup>[109]</sup> prepared MHAp using HAp and cobalt ferrite ( $\text{CoFe}_2\text{O}_4$ ), which had a rapid adsorption and total adsorption capacity of 338 mg/g for uranium. In both studies by Ou *et al.*<sup>[109]</sup> and El-Maghrabi *et al.*<sup>[87]</sup>, the mechanism responsible for uranium capture was also complex formation with MHAp. Furthermore, both types of MHAp could be separated from the uranium-MHAp complex by magnetic separation, proving the

remarkable regenerability of both types of MHAp. HAp composites have also been produced in the quest for developing an effective tool for uranium capture. The combined properties of HAp and functional groups of other components used in the composite can endow the composite with selective elimination of uranium. HAp/ZIF-67 composites developed by Xuan *et al.*<sup>[110]</sup> exhibited a high adsorption capacity of 453.1 mg/g for uranium, with a uranium capture efficiency of 97.29%. Ji *et al.*<sup>[111]</sup> recently developed HAp-modified polyethylene imine/carbon nanotube (PEI/CNT) composite displayed an adsorption capacity for uranium of more than twice of HAp. Natural materials may also be incorporated into HAp composites to enhance the eco-friendliness of the nuclear waste management system. Saha *et al.*<sup>[112]</sup> impregnated alginate (Alg) beads with HAp-coated activated carbon (AC) as a sorbent for removing uranium from water. Alg/HAp/AC beads possessed a sorption capacity of 18.66 mg/g with a uranium removal efficiency greater than 92%. HAp/biocarbon composites synthesised by Liao *et al.*<sup>[113]</sup> had a high selectivity for uranium and its composites, and had a maximum static and dynamic adsorption capacity of 834.8 mg/g and 782.8 mg/g respectively for uranium. HAp/biochar nanocomposites fabricated by Ahmed *et al.*<sup>[114]</sup> had a maximum adsorption capacity for uranium of 428.25 mg/g. The adsorption of uranium onto the HAp/biochar nanocomposites was spontaneous and endothermic. Initial rapid adsorption of uranium occurred before rate-limited sorption of uranium via surface complexation and diffusion. The HAp/biochar nanocomposites also demonstrated good recyclability by retaining a uranium adsorption capacity above 90% after five regeneration cycles.

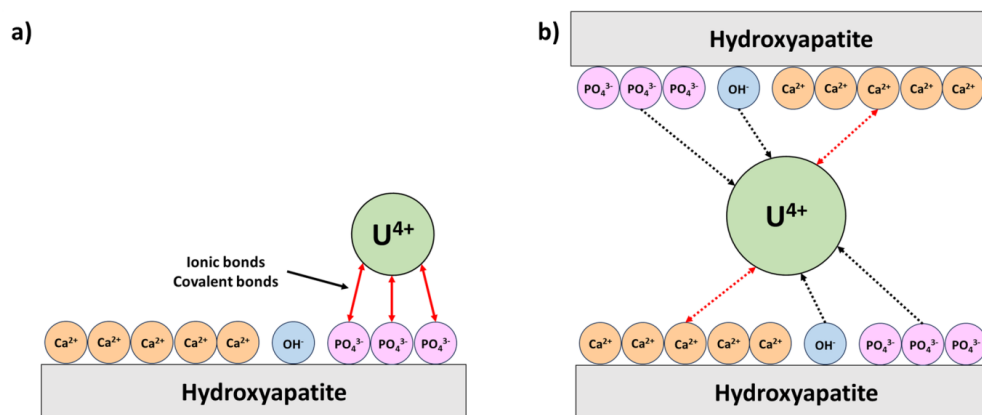


**Figure 4.** A schematic diagram of (a) chemisorption and (b) complex formation between uranium and hydroxyapatite

Intricate architectures of HAp have also recently shown potential as new methods for uranium capture. These architectures possess a high surface-area-to-volume ratio to maximise the contact area between HAp surface and nuclear waste for efficient uranium capture<sup>[115]</sup>. Wu *et al.*<sup>[116]</sup> fabricated hierarchical HAp microspheres with a specific surface area of 182.6 m<sup>2</sup>/g and pore size of 10.5 nm. These hierarchical HAp microspheres could rapidly adsorb uranium via chemisorption and complex formation, with a maximum adsorption capacity of 199 mg/g. Ma *et al.*<sup>[117]</sup> developed HAp microtubes with a specific surface area of 10.8 m<sup>2</sup>/g, pore size of 13.0 nm and maximum adsorption capacity for uranium of 356.42 mg/g for uranium capture. Despite exhibiting a uranium capture efficiency above 98.76% and rapid adsorption of uranium, the adsorption of uranium onto the HAp microtubes is inhibited by fulvic acid, magnesium and sulfate ions.

Furthermore, a myriad of HAp aerogels have recently been produced for nuclear waste management. Aerogels are light and mechanically robust structures with a continuous pore network that provides more active sites for adsorption of uranium onto HAp. Xiong *et al.*<sup>[118]</sup> developed HAp/konjac gum (KGM) aerogels via freeze-drying calcination (FDC) for uranium capture. The HAp/KGM aerogel had a maximum adsorption capacity for uranium of 2087.6 mg/g with a uranium removal efficiency of 99.4% within 10 min. The HAp/KGM aerogel was predicted to immobilise uranium through ion exchange, adsorption, or dissolution-

precipitations (see **Figures 4 and 5a**). A HAp-modified coal fly ash aerogel (CFAA) developed by Huang *et al.*<sup>[119]</sup> exhibited a uranium capture efficiency of 97.6% and maximum adsorption capacity of 205.7 mg/g. The uranium capture efficiency of HAp/CFAA remained above 80% after five regeneration cycles. The uranium capture mechanism of HAp/CFAA was also predicted to be surface complexation, ion exchange or dissolution-precipitation. Xiong *et al.*<sup>[120]</sup> also developed HAp/xanthan gum (XG) and HAp/chitosan aerogels for uranium immobilisation. However, the HAp/XG and HAp/chitosan aerogels displayed a significantly poorer performance than their HAp/KGM aerogel counterparts in uranium immobilisation. HAp/KGM aerogels prepared by Wang *et al.*<sup>[121]</sup> had a maximum adsorption capacity of 2055.2 mg/g and uranium capture efficiency of 99.4%. Dissolution-precipitation was predicted to be responsible for the efficient uranium capture of this HAp/KGM aerogel. HAp/kaolin (KL) aerogels were also developed by Xiong *et al.*<sup>[122]</sup>, which was postulated to have a uranium capture mechanism of either ion exchange, chemisorption, surface complexation or electrostatic adsorption (see **Figure 5b**). HAp/KL aerogels had remarkable recyclability, with uranium capture efficiency of 93.4% and maximum adsorption capacity of 401.6 mg/g. While HAp aerogels are currently an expensive method for nuclear waste management, they exhibit immense potential as a tool for radioactive waste management<sup>[118]</sup>.

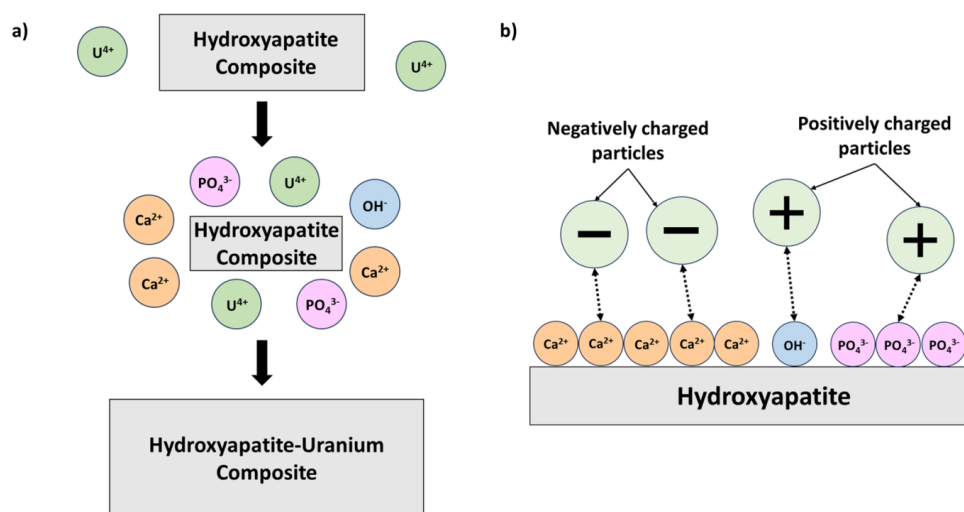


**Figure 5.** A schematic diagram of (a) dissolution-precipitation between uranium and hydroxyapatite and (b) electrostatic adsorption between charged particles and hydroxyapatite



## 5. Coatings and Surface Treatments

### 5.1 Anti-Corrosive Agents

HAp was initially shown to cause surface passivation by reacting with metallic surfaces to form a metallic phosphate layer. The metallic phosphate layer possesses excellent barrier properties that prevents the metallic surface from reacting with corrosive substances. This surface passivation phenomenon enables HAp to be employed for corrosion protection applications<sup>[123]</sup>. Later studies by Guo *et al.*<sup>[124]</sup> showed that HAp also prevents corrosion by increasing the diffusion path of corrosive agents. The diffusion path of corrosive agents through HAp-based anti-corrosive layers changes depending on the HAp crystal facet exposed to the corrosive agent. This unlocks the frontier for tuning HAp-incorporated anti-corrosive agents by controlling the crystallinity of HAp. The anti-corrosive mechanisms of HAp are shown in **Figure 6**. HAp can also be doped to improve its anticorrosive properties. HAp composites have also displayed anti-corrosive properties owing to the presence of HAp. A study by Cheng *et al.*<sup>[125]</sup> has demonstrated that polydopamine (PDA)-doped HAp nanosheets are an effective anti-corrosive material when integrated within an epoxy matrix. Interactions between HAp and PDA chelate

and inhibit diffusion of corrosive agents through the epoxy-PDA-HAp layer, shielding the metal surface from corrosion. Zhou *et al.*<sup>[126]</sup> confirmed that the interactions between PDA and HAp are responsible for the excellent anticorrosive properties of PDA-HAp corrosion protection layers. Moreover, PDA-HAp composites with a layered structure developed by Zhou *et al.*<sup>[126]</sup> have a dense packing that also improves its anticorrosive properties. PDA-HAp also serves as a matrix for carrying other anti-corrosive substances. Guo *et al.*<sup>[127]</sup> developed anti-corrosive agents using PDA-HAp loaded with silane/alumina (KH550/Al<sub>2</sub>O<sub>3</sub>) nanoparticles, which displayed both aforementioned corrosion protection mechanisms. KH550/Al<sub>2</sub>O<sub>3</sub> nanoparticles are also anti-corrosive agents. The PDA-HAp composite first displayed barrier properties to protect the metal surface from corrosive substances. During the corrosion protection, the PDA-HAp composite corroded instead of the metal surface. After the PDA-HAp layer was sufficiently corroded, it acted as a corrosion inhibitor by extending the diffusion path of the corrosive agents. Finally, KH550/Al<sub>2</sub>O<sub>3</sub> nanoparticles were released from the PDA-HAp matrix to reinforce the corrosion inhibition and protect the metal surface.

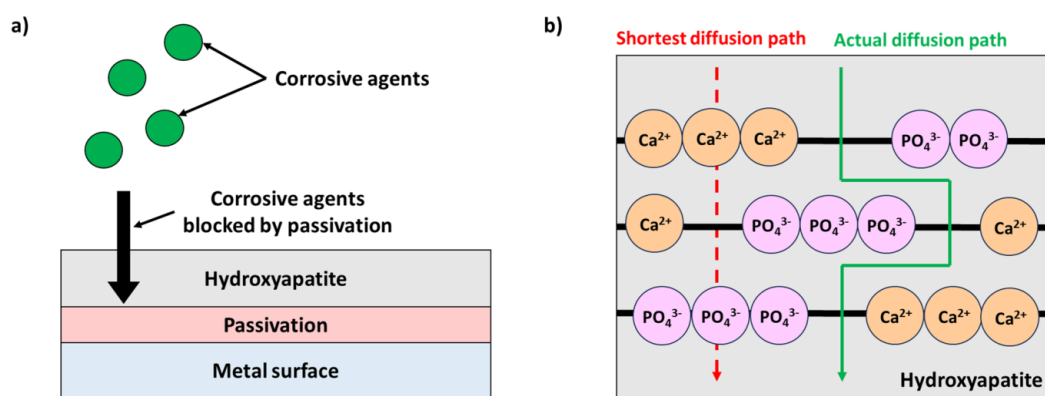


**Figure 6.** Schematic diagrams of the mechanism of corrosion protection by hydroxyapatite via (a) passivation and (b) diffusion path extension through crystal planes

Recently, the development of anti-corrosive coatings containing HAp have begun to gain popularity. Anti-corrosion pigments are liquid, insoluble substances that can easily be applied onto surfaces for corrosion protection. Xu *et al.*<sup>[128]</sup> fabricated a ZnO-HAp-epoxy pigment to function as anti-corrosive agents to protect the hull of marine vessels from corrosion due to NaCl. The ZnO-HAp-epoxy pigment exhibited the best anti-

corrosive properties when the mass of ZnO was 1.857 times the mass of HAp. ZnO adhered to HAp to form a hydrophobic complex that inhibits the diffusion of corrosive substances through the matrix. Ion exchange between chloride ions and the hydroxide ions in HAp also occurred to form chlorapatite, extending the service life of the anti-corrosive ZnO-HAp-epoxy pigment. Xue *et al.*<sup>[129]</sup> prepared HAp/graphene oxide

(GO) pigments via in situ bonding for industrial metal protection from NaCl. HAp/GO pigments prevent corrosion via 3 methods: initial corrosion protection by HAp/GO acting as a barrier between the metal surface and NaCl, ion exchange between chloride and hydroxide ions to form chlorapatite, and surface passivation by interaction between HAp and the metal surface. This threefold anti-corrosion mechanism endows HAp/GO pigments exceptional corrosion protection properties. Work by Xu *et al.*<sup>[128]</sup> and Xue *et al.*<sup>[129]</sup> demonstrates how interactions between HAp and oxides can produce enhanced anti-corrosive effects compared to HAp. However, more studies are required to understand the properties of oxides required to interact with HAp to enhance its anti-corrosive properties in natural environments. Furthermore, HAp's biocompatibility and non-toxicity allows it to be environmentally friendly to flora and fauna when it is applied as a corrosion protection layer on metal surfaces exposed to nature. As such, HAp-based anti-corrosive agents are particularly beneficial in applications where metal structures are exposed to natural environments for long periods of time.

### 5.2 Antimicrobial Food Packaging

Apart from HAp's ability to be utilised as corrosion

protection, HAp has also been explored for various antimicrobial coating applications beyond the biomedical field due to its inherent antibacterial properties<sup>[130]</sup>. HAp is hydrophilic because of the presence of hydroxyl groups on its surface, which diminishes microbial cell adhesion on the surface of HAp. The electrostatic repulsion between negatively-charged microbial cell walls and phosphate groups on the surface of HAp further reduces microbial cell adhesion onto HAp. Thus, HAp coatings can prevent the growth of bacteria and other microorganisms, making them useful in a range of industries to improve hygiene and prevent the spread of infections<sup>[131]</sup>. These coatings can prevent the growth of bacteria and other microorganisms, making them useful in a range of industries to improve hygiene and prevent the spread of infections. HAp has an innate low antibacterial activity towards *Escherichia coli* (E.coli)<sup>[132]</sup>. Pristine HAp appears to be bacteriostatic, inhibiting the growth of microbes. The possible mechanism of bacteriostasis is illustrated in **Figure 7a**. HAp nanoparticles incorporated into polypropylene (PP) food packaging significantly inhibited the growth of psychrophilic, yeasts, and molds bacteria compared to pristine PP packaging<sup>[133]</sup>.

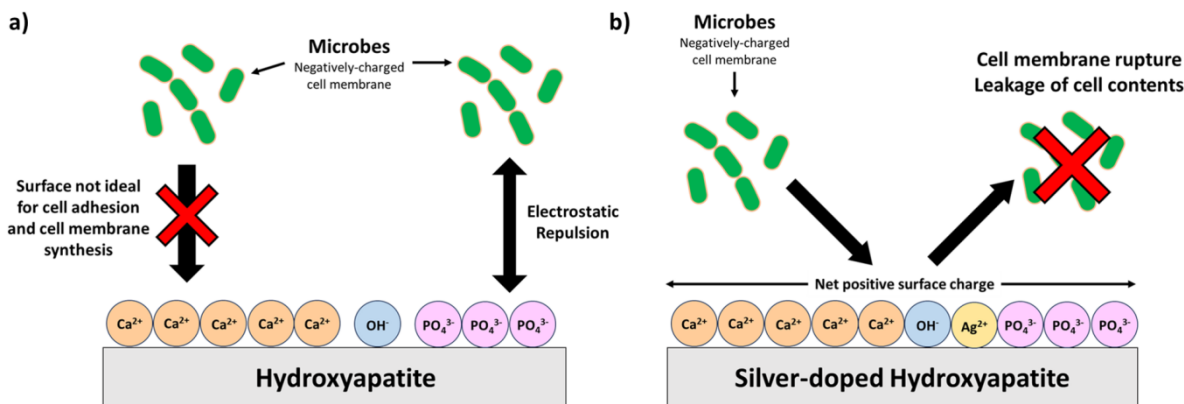


**Figure 7.** Schematic diagrams of the (a) bacteriostatic and (b) bactericidal mechanisms of antimicrobial activity in hydroxyapatite and silver-doped hydroxyapatite

Ag-HAp is bactericidal (see **Figure 7b**) was found to have superior antimicrobial properties than pristine HAp. The positive surface charge of Ag-HAp experiences strong electrostatic attraction with the negatively-charged bacteria cell walls. The strong electrostatic attraction increases the permeability of the bacteria cell membrane. The presence of silver

ions also results in the denaturation of the bacterial cell membrane. The increased permeability and denatured cell membrane eventually leads to rupture of the cell membrane and leakage of cell contents, killing the bacteria cell<sup>[134]</sup>. A study by Sinulingga *et al.*<sup>[132]</sup> demonstrates that Ag-HAp has an antimicrobial activity of 61% against E.coli, compared to the 12%

antimicrobial activity of pristine HAp. Sinulingga *et al.*<sup>[132]</sup> also found that co-doping HAp composite with silver and zinc or silver and magnesium results in a 99% killing rate of *E.coli*. Such excellent antimicrobial activity arises due to increased electrostatic interactions between metal ions and the bacterial wall membrane, causing the cell membrane to rupture and leakage of cell contents<sup>[135]</sup>. The outstanding antimicrobial properties of doped HAp make it a possible fixture as a component in antimicrobial food packaging. Polyhydroxyethylmethacrylate (PHEMA)-doped HAp developed by Gökmen<sup>[136]</sup> could form a porous film with excellent barrier properties. The PHEMA-HAp films successfully preserved the colour, shape and size of cherry tomatoes with no signs of antimicrobial growth on the cherry tomatoes.

HAp also serves as a non-toxic carrier for antimicrobial agents in food packaging. The porous structure of HAp allows substances to be contained within the porous network, allowing HAp to act as a carrier for antimicrobial agents. Malvano *et al.*<sup>[137]</sup> fabricated edible coatings containing HAp, alginate (Alg) and quercetin. The HAp/Alg/quercetin coatings displayed desirable antimicrobial properties by inhibiting the growth of gram negative *Pseudomonas fluorescens*. Further investigations by Malvano *et al.*<sup>[138]</sup> discovered that the HAp/Alg/quercetin effectively inhibits the growth of gram negative *Pseudomonas aeruginosa*, which is the bacteria strain responsible for food spoilage during storage. The HAp/Alg/quercetin coating had the lowest total viable bacteria count (TVC), psychotropic bacteria, *Enterobacteriaceae* and *Pseudomonas aeruginosa* among the different coatings they examined. Wang *et al.*<sup>[139]</sup> developed polyvinyl alcohol (PVA)/sesbania gum (SG) films containing tea tree oil (TTO)-loaded HAp microspheres as a basis for active food packaging. The PVA/SG/HAp/TTO films exhibited bacteriostatic properties, having a stronger antimicrobial effect against gram positive *Staphylococcus aureus* (*S. aureus*) than gram negative *E.coli*. As seen, HAp itself is likely to be weakly bacteriostatic, yet dopants or composites can confer HAp bactericidal properties. This is crucial in the food and beverage industry as protection of food from microbial contamination is vital for ensuring that they remain safe for human consumption. Bactericidal HAp-incorporated coatings may also assist in maintaining

nutritional value, retaining the quality and flavour of food produce, and reducing the risk of foodborne illnesses.

## 6. Flame Retardants

Flame retardants are an important safety aspect in modern life, being incorporated into many electronic devices and plastic products that could present a fire hazard. HAp is an attractive material for flame retardants since it is non-toxic to humans, which can mitigate the adverse health effects that arise when flame retardant particles bioaccumulate in humans during fire extinguishing<sup>[140]</sup>. On its own, HAp possesses flame retardant properties due to its high heat resistance and thermal stability. HAp's stoichiometric Ca/P ratio of 1.67 is responsible for its excellent thermal stability and heat resistance. At deviations of the Ca/P ratio below 1.67, secondary calcium phosphate phases are formed that accelerate its thermal decomposition when heated. Meanwhile at deviations of the Ca/P ratio above 1.67, calcium oxide forms when the calcium phosphate is heated above 900 °C. Calcium oxide reacts with the atmosphere to form calcium hydroxide or calcium carbonate when cooled, which accelerates the decomposition of the calcium phosphate. HAp does not undergo these decomposition pathways at high temperatures, allowing it to absorb heat and prevent the spread of fire<sup>[141]</sup>. The action of HAp flame retardants is illustrated in **Figure 8**. The excellent flame retardance of HAp spearheaded the creation of ultralong HApNW flame retardant paper. The ultralong HApNW paper displays excellent flame retardance, and maintains its mechanical and structural integrity at high temperatures<sup>[142]</sup>. HAp nanowire papers were also incorporated into a smart fire alarm wallpaper system because of its high heat resistance and flame retardance<sup>[143]</sup>. HAp has also been shown to endow excellent flame retardancy to composite materials. Vahabi *et al.*<sup>[144]</sup> developed a HAp/carbon nanotube (CNT)/ammonium polyphosphate (APP) flame retardant for poly(ethylene-co-vinyl acetate) (EVA). HAp/CNT/APP exhibited superior flame retardancy compared to pristine APP, which is a conventional flame retardant for EVA. The presence of HAp decreased the heat release rate (HRR) of the APP flame retardant on EVA, and achieved a peak HRR of 212 kW/m<sup>2</sup> compared to pristine APP's peak HRR

of 335 kW/m<sup>2</sup>. A superamphiphobic coating of HAp, fluorine and SiO<sub>2</sub> was fabricated by Ai *et al.*<sup>[145]</sup> that displayed good flame retardancy and oil resistance. Czlonka *et al.*<sup>[146]</sup> fabricated a polyurethane (PU)/HAp/lavender residue (LR) as a novel halogen-free flame retardant. PU/HAp/LR composites had a peak HRR of 130 kW/m<sup>2</sup>, while PU and PU/LR had peak HRRs of 203 kW/m<sup>2</sup> and 263 kW/m<sup>2</sup> respectively. The significant decrease of peak HRR after the addition of HAp into PU/LR is a testament to the excellent flame retardance of HAp. Nihmath *et al.*<sup>[147]</sup> investigated the influence of HAp nanoparticles on the flame retardance

of chlorinated nitrile rubber (Cl-NBR)/chlorinated ethylene-propylene-diene (Cl-EPDM) rubber nanocomposites. The limiting oxygen index (LOI) of HAp/Cl-NBR/Cl-EPDM increases as HAp content increases, which is indicative of the enhancement of the flame retardance of HAp/Cl-NBR/Cl-EPDM by HAp. Polar interactions between HAp and the Cl-NBR or Cl-EPDM segments give rise to a highly physically-crosslinked structure that further increases the thermal stability and flame retardance of HAp/Cl-NBR-Cl-EPDM.

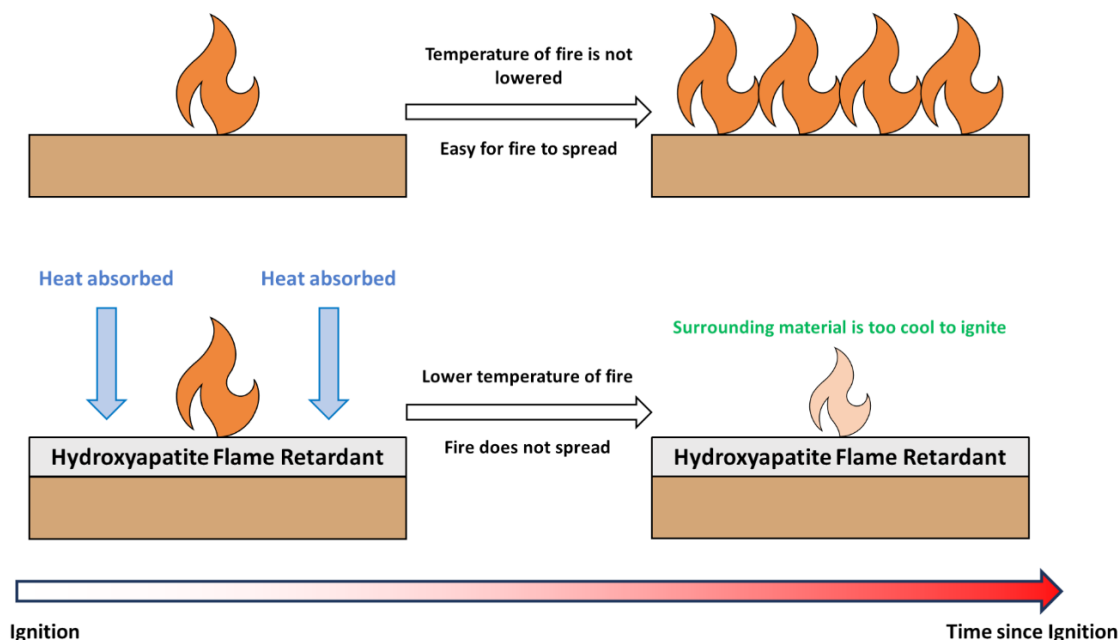


Figure 8. Schematic diagram showing the mechanism of hydroxyapatite flame retardants

Recent developments in flame retardants focus on improving the non-toxicity and environmentally-friendliness of the flame retardants. Flame retardants may produce toxic and harmful products during fire extinguishing or by reactions to the environment they are exposed to. Hence, it is imperative for flame retardants to be non-toxic and environmentally friendly. HAp, being a natural material, is environmentally-friendly and non-toxic, making it an attractive candidate for producing environmentally-friendly flame retardants. Zhou *et al.*<sup>[148]</sup> fabricated a hybrid HApNW flame retardant (f-HApNW) using HAp, dopamine (DA), 3-aminopropyltriethoxysilane (APTES) and hexachlorocyclotriphosphazene (HCCP)-crosslinked polyphosphazene (PPHOS). The f-HApNWs were

deployed as flame retardants for unsaturated polyester (UPR). f-HApNW had a maximum total heat release (THR) of 91.2 MJ/m<sup>2</sup> and minimum peak carbon monoxide production rate (PCOP) of 0.015 g/s, while decreasing the peak HRR of UPR from 818.2 kW/m<sup>2</sup> to 650.5 kW/m<sup>2</sup>. The inhibition of CO production by f-HApNW decreases the toxicity of the smoke produced during pyrolysis. Furthermore, f-HApNW produces phenolic compounds during thermal degradation, which act as free radical scavengers to reduce the fuel supply to the fire<sup>[148]</sup>. HAp and other natural materials can be integrated together to produce non-toxic and potentially renewable flame retardants. Huang *et al.*<sup>[149]</sup> developed a HAp/calcium alginate (CaAlg) hybrid flame retardant material via a green



sol-gel method. The excellent flame retardancy of the HAp/CaAlg was predicted to arise from HAp facilitating the carbonization of HAp/Ca/Alg. A HAp/sodium alginate (NaAlg) aerogel flame retardant developed by Zhu *et al.*<sup>[150]</sup> had a thermal insulation of 35.15 mW/mK and smoke gas release of 11.3 m<sup>2</sup>/m<sup>2</sup> on top of its excellent flame retardant properties. The NaAlg aerogel flame retardant also possessed robust mechanical properties due to its double-crosslinked structure, with a maximum compressive strength of 0.75 MPa and Young's Modulus of 2.39 MPa. This NaAlg aerogel flame retardant highlights the prospect of producing mechanically robust flame retardants using natural materials. Zhu *et al.*<sup>[151]</sup> has prepared a chitosan aerogel/HAp monolith that exhibited remarkable flame retardance. The directional freezing used to create the chitosan aerogel/HAp monolith was responsible for the low density, high porosity and unidirectional microtubule pore structure of the monolith. Heat conduction and thermal resistance, and hence flame retardance, arises from the highly orientated pores and HAp nanocrystals in chitosan aerogel/HAp monolith. Interestingly, a bilayer flame retardant made entirely from natural materials has been developed by Nabipour *et al.*<sup>[152]</sup> from HAp, NaAlg and chitosan. Bilayers of HAp/NaAlg and HAp/chitosan coated onto PU decreased THR by 56.5%, peak HRR by 77.7% and smoke reduction by 53.8%. These developments show that HAp could be a vital material for constructing novel non-toxic and flame retardants with abundant, renewable natural materials.

## 7. Energy Storage and Conversion

### 7.1 Electrical Insulators

HAp displays electrical insulation properties due to its wide intrinsic bandgap, which has motivated many researchers to develop HAp-containing electrical insulators in recent years<sup>[153]</sup>. HAp has exhibited its effectiveness in enhancing the electrical insulating properties of composites. Wang *et al.*<sup>[153]</sup> developed an electrical insulating composite paper consisting of ultralong HApNWs and aramid nanofibers (ANF), both of which are excellent electrical insulators. The HApNW/ANF composite had a dielectric breakdown strength of 92.4 kV/mm alongside excellent mechanical properties arising from the interfacial interactions and physical entanglement of

the HApNWs and ANFs. HApNWs reinforced the electrical insulating and mechanical properties of ANFs, leading to the remarkable dielectric breakdown strength and mechanical properties displayed by the HApNW/ANF composite. A study by Huang *et al.*<sup>[154]</sup> showed that HApNWs successfully enhanced the electrical insulating properties of hydroxyethyl cellulose (HEC) composites. The strong interactions between HApNWs and HEC prevented the HApNW/HEC from decomposition under high current flow. The HApNW/HEC composites attained a maximum dielectric breakdown strength of 12.7 kV/mm. Interestingly, ultralong HApNW pulp synthesized by Dong *et al.*<sup>[155]</sup> displayed attractive electrical insulation properties, with a dielectric strength of 15.7 kV/mm and electrical resistivity of  $6.3 \times 10^8 \Omega\text{m}$ . HApNW pulp appears to be a promising avenue for the exploration of developing HAp-based electrical insulators, rather than using HAp as a reinforcing agent for the electrical insulating properties of electrically insulating materials.

### 7.2 Electrochemical Cells

Interestingly, HAp is also a viable material in energy storage and conversion. HAp exhibits good proton conductivity, which is vital for the facilitation of charge transfer. HAp has attractive ion exchange and catalytic activity for electrochemical cells and energy storage applications. The large surface area and hydrophilicity endows HAp sufficient active sites for electrochemical reactions and interaction with electrolytes. Moreover, HAp is an environmentally friendly and nontoxic material with excellent thermal stability, mechanical properties and fire resistance, making it an attractive material for the construction of sustainable, eco-friendly energy devices<sup>[156]</sup>. Electrochemical cells consist of an anode and cathode, each in contact with different electrolytes. A porous separator prevents the electrolytes from coming into contact with each other. A study by Wen *et al.*<sup>[157]</sup> demonstrated that HAp can be incorporated into lithium ion batteries (LIB) to enhance the ionic conductivity of polyethylene oxide (PEO) solid state electrolytes (SSE). Liang *et al.*<sup>[158]</sup> employed HAp as a filler for PEO, which resulted in improved ionic conductivity of the SSE. HAp facilitated lithium salt dissociation with minor dissociation energy due to the electrostatic attraction between lithium ions and the negative surface charge

of HAp. Xi *et al.*<sup>[159]</sup> incorporated HAp nanowires into PEO SSE and discovered that HAp nanowires could regulate the dissociation and diffusion of lithium ions, and inhibit superoxide radicals in PEO. HAp has been incorporated into the separators of electrochemical cells to confer compositional and structural stability to the separators at high operating temperatures, and to enhance electrochemical performance and cycle stability. A study by Rao *et al.*<sup>[160]</sup> demonstrated that HAp nanowires can act as a separator in LIB while Li *et al.*<sup>[161]</sup> developed a HAp nanowire composite based on aramid fibre paper that resulted in improved electrochemical performance of lithium-sulfur batteries (LSB). A HAp/porous carbon composite developed by Wang *et al.*<sup>[162]</sup> facilitated the reduction and enhanced the redox kinetics of lithium polysulfides in LSB. The HAp/porous carbon composites displayed a low capacity fading rate of 0.051% and had a specific capacity of 815 mAh/g at 0.5 C after 325 cycles. Saroja *et al.*<sup>[163]</sup> designed a quasi-solid state gel polymer electrolyte containing HAp (HAp/GPE) that also displayed potential to be a replacement for glass fibre separators in next generation sodium ion batteries (SIB). The HAp/GPE had a porosity of 64%, an ionic conductivity of  $1.086 \times 10^{-3}$  S/cm, high electrolyte uptake and maximum electrochemical stability of 4.9 V. The SIB containing HAp/GPE exhibited a superior capacitance and higher current density than conventional SIBs containing liquid electrolytes and a glass fibre separator. The excellent thermal stability and flame retardance of HAp can be incorporated into composite separators containing HAp without compromising electrochemical performance. Rao *et al.*<sup>[164]</sup> fabricated a composite LSB separator using HAp, manganese(II,III) oxide ( $\text{Mn}_3\text{O}_4$ ) and CNT. The HAp/ $\text{Mn}_3\text{O}_4$ /CNT separator possessed excellent thermal stability, enhanced lithium plating at the anode and suppressed polysulfide dissociation at the cathode. Electrolyte combustion was suppressed because of the excellent thermal stability of HAp. The LSB containing HAp/ $\text{Mn}_3\text{O}_4$ /CNT separator had an initial capacity of 1319 mAh/g and maintained a capacity of 1000 mAh/g after 150 cycles. Hou *et al.*<sup>[165]</sup> also recently produced a bifunctional separator comprised of HAp, poly(vinylidene fluoride-co-hexafluoropropylene) (PVDF) and MXene that exhibited superior flame retardance and enhanced overall electrochemical cell performance

of LIB compared to a traditional PP LIB separator. The development of separators made using HAp and other natural materials is gaining popularity due to the demand for eco-friendly electrochemical cells. Liu *et al.*<sup>[166]</sup> fabricated a hybrid HAp/cellulose LIB separator that displayed excellent flame retardance and thermal stability. The HAp/cellulose separators also had superior electrolyte wettability than traditional PP separators in LIB. A polyacrylonitrile (PAN), cellulose acetate (CA) and HAp composite separator produced by Chen *et al.*<sup>[167]</sup> had excellent ionic conductivity, with an electrolyte uptake rate of 281%. The PAN/CA/HAp separator had excellent thermal stability, displaying no significant deformation in an environment at 200 °C for 35 min. PAN/CA/HAp separator also had good cycle stability with a capacity of 157.6 mAh/g after 50 cycles at 0.5 C.

### 7.3 Supercapacitors

HAp is also used in the production of supercapacitors (SCs). SCs are energy storage devices used in applications that require rapid charge/discharge cycles at high voltages. SCs comprise porous electrodes, each in contact with a current collector separated by an electrolyte. A permeable membrane facilitates charge transfer within the electrolyte. Selvam *et al.*<sup>[168]</sup> recently fabricated a composite electrode with HAp, polyvinylpyrrolidone (PVP), manganese(II) oxide ( $\text{MnO}_2$ ) and manganese(II) carbonate ( $\text{MnCO}_3$ ) for high temperature SC applications. The SC containing HAp/PVP/ $\text{MnO}_2$ @ $\text{MnCO}_3$  electrode possessed a maximum capacitance of 409.5 F/g. The resulting SC had a specific capacitance of 126 F/g at 400 °C. The SC also retained 90% of its capacitance after 100,000 charge/discharge cycles. While composites remain promising for enhancing SC performances, the demand for green and eco-friendly electronic devices spearheads the advancement of SCs away from complex composites that usually require non-eco-friendly materials to construct. Biosupercapacitors (BSCs) are SCs constructed using biomass-derived materials and are gaining popularity because of their eco-friendliness. Porous BSC electrodes can be produced using the porous structure of HAp as a template<sup>[169]</sup>. Porous nitrogen-containing carbon materials (NCCMs) derived from the pyrolysis of biomass are cheap, possess robust mechanical properties and conductivity, and can easily be doped onto HAp. Studies by Chu *et*

*al.*<sup>[170]</sup> highlight that HAp prevents the sublimation of 1,10-phenanthroline during the production of NCCMs and promotes the formation of oxygen-rich carbonyl groups on the surface of the NCCMs. The oxygen-rich carbonyl groups are responsible for NCCM-doped HAp (NCCM-HAp) having a specific capacitance of 366 F/g at 0.5 A/g. NCCM-HAp enables oxidative coupling of amines to imines with a yield of 84%-95%. NCCM-HAp also possesses a capacitance retention of 98.5% after 1000 charge/discharge cycles at 10 A/g<sup>[170,171]</sup>. HAp has also been used as a template to construct porous NCCM-HAp electrodes with a hierarchical structure (NCCM-HAp-h). Hierarchical structures provide a greater specific surface area to the NCCM electrodes for enhanced BSC performance. Chitin-derived NCCMs were synthesised by Chu *et al.*<sup>[171]</sup> and used to construct NCCM-HAp-h. NCCM-HAp-h had a specific capacitance of 346 F/g at a current density of 0.5 A/g, and retained 92% of its capacitance after 5000 charge/discharge cycles. Furthermore, a BSC containing NCCM-HAp-h successfully stored energy from sunlight before converting it to electrical energy in a light emitting diode (LED). NCCM-HAp-h fabricated by Lv *et al.*<sup>[172]</sup> using HAp and chitosan displayed a specific capacitance of 306.4 F/g and retains 93% of its capacitance after 10,000 cycles, while also being able to enable the operation of LEDs. Recently a study by Li *et al.*<sup>[173]</sup> used HAp as a carrier for zwitterionic silane (ZSi) as an additive for carboxylated chitosan (CCS) electrolytes in SCs. The HAp-ZSi additive successfully enhanced the ionic conductivity and mechanical strength of the CCS electrolytes. CCS/HAp-ZSi electrolyte improved the capacitance of SCs by up to 20% and retains 98% capacitance after 5000 cycles at 6mA/cm<sup>2</sup>.

## 8. Bioinspired Hydroxyapatite Materials

Bioinspired HAp materials (BHAp) are a new class of materials that combines the intrinsic properties of HAp with the hierarchical structure of natural polymeric materials to create composite materials with superior properties than existing HAp composite materials. The fabrication of BHAp requires the biomineralization of HAp onto a precursor, before incorporating the biomineralized precursor into a polymer network. BHAp possesses superior mechanical strength and toughness to HAp, which is

brittle. BHAp fabricated by biomineralization of HAp onto collagen has been investigated for its suitability for bone regeneration applications<sup>[174]</sup>. BHAp produced using a template copolymer of polystyrene (PS) and polydimethylsiloxane (PDMS) displayed remarkable mechanical properties owing to its layer-by-layer self-assembly<sup>[175]</sup>. Recently, Bai *et al.*<sup>[176]</sup> used HAp and poly(methyl methacrylate) (PMMA) to fabricate a HAp/PMMA BHAp with a nacre-mimicking structure. The HAp/PMMA BHAp possessed excellent mechanical properties owing to its high ceramic content. Qi *et al.*<sup>[177]</sup> demonstrated the successful biomineralization of HAp onto cellulose using a poly(acrylic acid) (PAA) precursor. The resulting HAp/cellulose BHAp possessed a similar structure to natural bone due to its fibrillar and hierarchical structure. Cellulose nanocrystal (CNC)/HAp composites were successfully produced via in situ coating of HAp onto CNCs. HAp reinforced the mechanical properties of the CNC/HAp composites, which allowed the layer-by-layer assembly of CNC/HAp with chitosan and hyaluronic acid to produce a potentially biocompatible and sustainable bone scaffold<sup>[178]</sup>. HAp-reinforced alginate gels contained a bone-mimicking, fibrous, anisotropic hierarchical structure and was predicted to have a multiscale reinforcing mechanism because of the presence of HAp within the gel network<sup>[179]</sup>. Overall, research on BHAp synthesised with polymeric templates focuses on combining the properties of HAp with the attractive properties of the polymer template for biomedical applications.

Aside from hybrid polymeric BHAp, HAp produced using biogenic calcium sources (BCS) are also classified as BHAp. Synthesis of BHAp from BCS allows the retention of the naturally produced, highly ordered natural crystal orientation of the BCS. This highly ordered crystal orientation is responsible for the enhanced biomimicry and properties of BHAp compared to synthetic HAp. Gomez-Vasquez *et al.*<sup>[180]</sup> synthesised BHAp from eggshells via a wet-chemical precipitation method. The eggshell-derived BHAp had a 35% smaller crystal size and crystal size distribution compared to synthetic HAp, which makes it promising for applications in guided bone regeneration. BHAp can also be produced using HAp as a precursor for bioinspired deposition of other materials. Fu *et al.*<sup>[181]</sup> fabricated vancomycin-loaded GO hydrogels

and inserted them into the porous network of HAp to create HAp/GO BHAp coatings. The HAp/GO BHAp coatings exhibited superior wear resistance, antimicrobial activity and self-lubrication properties compared to pristine HAp coatings. Furthermore, the HAp/GO BHAp coating also displayed sustained drug release behaviour. Mu *et al.*<sup>[182]</sup> developed a BHAp via bioinspired co-deposition of PDA and PEI onto HAp (HAp/PDA/PEI). The HAp/PDA/PEI BHAp was further used as reinforcement for a polysulfone (PSF) ultrafiltration membrane. The HAp/PDA/PEI BHAp was shown to improve the antifouling properties, while also enhancing the porosity and hydrophilicity of the PSF membrane. Interestingly, a BHAp of HAp and BaTiO<sub>3</sub> showed promise in becoming a new type of scaffold for bone tissue regeneration<sup>[183]</sup>. The prospect of creating BHAp with other ceramic or perovskite materials could spearhead the development of BHAp for high temperature applications. Nonetheless, recent developments of BHAp still lean towards utilising BHAp in biomedical applications, even with different fabrication methods and HAp sources.

## 9. Future Perspectives

### 9.1 Computers and Machine Learning

HAp potentially sees applications in the construction of next-generation computers for artificial intelligence (AI) and machine learning (ML). AI and ML are becoming increasingly sophisticated and complex as they get integrated into modern life. The complex algorithms that form the basis of AI and ML generate a large amount of heat from the computer running them. Modern computer parts are also built using rare, valuable and expensive materials such as gold, silver, platinum and palladium. These expensive materials make the recycling or disposal of computer parts a complicated and hazardous process. Meanwhile, a large amount of memory is also required for the algorithms to run. New generations of computers developed for AI and ML require parts with higher operating temperatures and higher memory storage<sup>[184]</sup>. HAp can be incorporated into composites to produce mechanically robust, fire-resistant computer parts with high operating temperatures. These HAp-containing composites will not experience structural or thermal deformation and maintain intended chemical and

physical properties at high temperatures. As such, computers built with HAp-containing composites may be able to run complicated AI and ML algorithms for longer durations. MHAp composites could also be used to construct memory storage in computers. MHAp-based computer memory (MHAp-Mem) could potentially have a high heat resistance and operating temperature. The amount of raw magnetic material required to construct MHAp-Mem will also be significantly less than in conventional computer memory. MHAp-Mem could also allow high power computing and training of complex ML models for long periods of time, where large amounts of heat will be generated. On top of increasing operating temperatures, the incorporation of HAp or MHAp into computers also reinforces their flame retardance in a scenario where the computer may catch fire from prolonged use. Furthermore, utilising HAp to make computers further increases the eco-friendliness and recyclability of the electronic waste when the computer is disposed of. HAp, being a natural material, is nontoxic to the environment, making HAp-incorporated electronic waste more eco-friendly. Materials used for doped HAp or HAp complexes can be recovered together with HAp and separated from HAp to construct new electronic parts. With the increasing demand for recyclable and eco-friendly electronics, HAp could be vital to not only producing eco-friendly computer parts but also electronic components that can be separated, reprocessed, and restructured for different devices.

### 9.2 Recyclable Immunoassays

HAp is also an attractive material candidate for recyclable immunoassays (IAs). IAs are tests to determine the presence or concentration of a target analyte, usually a protein, in a solution using antibodies. IAs consists of a plastic protective housing encapsulating a porous membrane containing antibodies. Antibodies are highly specific, and each antibody will only bind to a specific analyte. This specificity allows foreign substances such as pathogens to be eliminated by the antibodies. Labels are chemically conjugated to antibodies and produce a detectable signal when analytes are bound to antibodies, allowing easy identification and quantification of analytes in the solution. The



signal is only detectable when a minimum amount of analyte-antibody complexes is formed. IAs are single-use devices and are disposed of once they have been used, which generates a large amount of plastic waste. Antibodies from IAs displaying negative results are also disposed of since the analyte is absent from the fluid sample. The waste generation from IAs was evident during the recent coronavirus (SARS-CoV-2) pandemic<sup>[185]</sup>. HAp has the potential to be used as a membrane in IAs. HAp's ease of doping and porous structure may allow easy functionalization of antibodies onto the surface of HAp. This allows more antibodies to be loaded onto the HAp surface which helps with more signals to be detected easily and display a more accurate IA result. The porous structure of HAp could also allow the fluid sample to diffuse quickly through the HAp IA membrane, leading to less time before a detectable signal is produced. The insolubility of HAp also prevents substrate dissolution and reactions of HAp with analyte solutions. This could potentially allow HAp membranes from negative IAs to retain their structure after being flushed to separate the membrane from the fluid sample. The separated membrane can then be dried and reused in a new IA. Recyclable IAs reduce waste generated from HAp disposal, and the regeneration of HAp enables the construction of new pristine recyclable IAs without the need for synthesis or extraction of HAp from various sources. In this context, the recycling of IAs is strictly due to dissolution, followed by the regeneration of HAp membranes, antibodies, and labels. Recyclable IAs will also decrease the need for the production of pristine antibodies and labels, saving material resources needed for IAs. Overall, recyclable IAs with HAp membranes will result in less resources consumed, and less waste generated from disposed IAs.

### 9.3 Waste-Derived Bioplastic Composites

Plastics have become a fixture in modern life because of their versatility and tunability into forms that meet various needs. Majority of the plastics are derived from non-renewable petroleum sources and pose a threat to the environment because of their non-biodegradable nature. Incineration and landfills of plastic waste also result in the formation and release of harmful chemicals into the environment. Alongside plastic waste, food waste is another major contributor to global pollution. Large amounts of food waste are

produced every year. HAp is a naturally occurring material that provides structural support in bones and is easily found in bone remnants from food waste. Other than HAp in bones, food waste also contains other natural materials such as chitin, collagen, gelatin and pectin, which are also eco-friendly and could be valorised to produce novel waste-derived bioplastics (WBPs)<sup>[186]</sup>. Hence, the extraction of materials from food waste to produce plastic alternatives is an important quest for reducing environmental pollution from plastic and food waste. WBPs made entirely from combining HAp with other natural materials will be non-toxic and biodegradable. HAp is able to retain its innate properties after extraction from natural sources, which allows them to potentially be exploited to reinforce the mechanical and thermal properties of WBPs. With the inclusion of HAp into the polymer matrix of WBP, electrostatic interactions between HAp and charged functional groups in the polymer matrix may enhance the mechanical properties of WBP. HAp microparticles or nanoparticles incorporated into a polymer matrix have a large surface area to volume ratio. The HAp particles are able to absorb energy from stress onto the WBPs, increasing the resistance of WBPs to fracture. HAp wires or fibres used to reinforce WBPs distribute the stress throughout the WBP structure, which increases the resistance of WBPs to plastic deformation and fracture. Furthermore, HAp confers thermal stability to WBPs due to HAp's stoichiometric Ca/P ratio of 1.67. The structural reinforcement and thermal stability conferred to WBPs by HAp could allow WBPs to possess similar mechanical properties to non-biodegradable high density polyethylene (HDPE). Furthermore, WBPs are predicted to be much cheaper to produce than HDPE due to the abundance of natural materials found in food waste. The possibility of producing WBPs from food waste not only reduces the annual amount of disposed food waste, but also generates a sustainable amount of plastics to satisfy the growing demand for plastics. This would also help to achieve the idea of a circular economy (see **Figure 9**) where the life cycle of materials from disposed products are extended. As a result, materials in waste could be given a new life and the annual amount of waste produced will also be minimised.

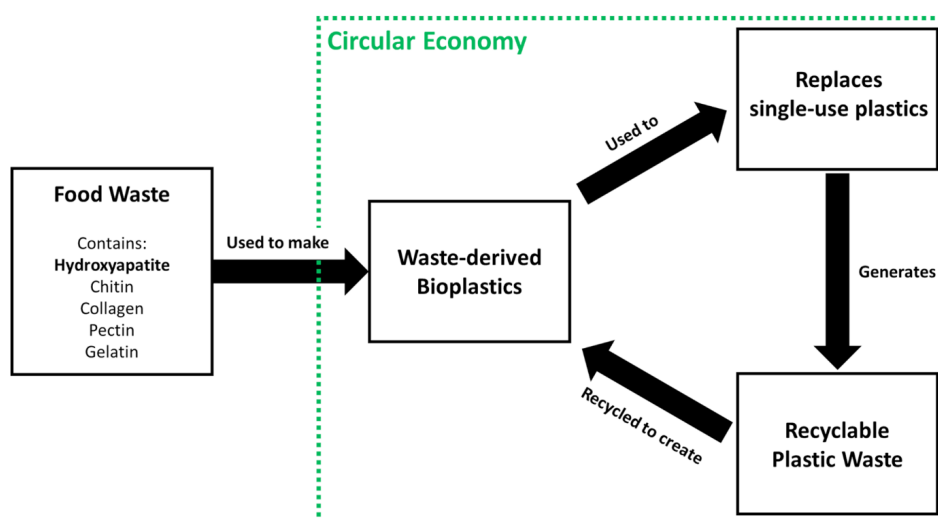


Figure 9. Concept of a circular economy of waste-derived bioplastics

## 10. Conclusion

In conclusion, this review highlights the applications of HAp in biomedical, bioimaging, separation and purification, catalysis, surface treatments and energy storage applications. Since HAp is a widely studied material in biomedical and bioimaging applications, more emphasis is given to the applications of HAp outside the biomedical field to showcase the outstanding versatility of HAp. Possible new applications of HAp for greener computer parts, recyclable immunoassays and waste-derived bioplastics are also proposed. However, the interactions between HAp and other relevant materials for novel green technologies need to be thoroughly investigated before HAp can be used in new applications. The structure-property relationships of HAp-based systems must also be analysed in order for a novel material system to be created. Currently, research surrounding HAp remains saturated by exploring the applications of HAp in biomedical applications. Research on HAp applications is slowly branching towards green and sustainability-focused applications. However, research on HAp remains overshadowed by research on other natural polymeric materials, such as alginate and cellulose, in the field of sustainability. While the amount of research work on BHAp is on the rise, it is mainly focused on utilising the hierarchical structure of natural materials to improve the performance of HAp in biomedical applications. Since HAp has demonstrated that it is a versatile, multifunctional material beyond biomedical applications, it is plausible that development of novel

green technologies in the near future will employ HAp as a reinforcing material. Yet in the long run, HAp is expected to take the mainstage in development of novel green technologies as its plethora of attractive properties are waiting to be rediscovered for future developments in purification technology, surface treatments, green electronics, and circular economies.

## Ethics Statement

Not applicable.

## Consent for publication

Not applicable.

## Availability of Supporting Data

Not applicable.

## Conflict of Interest

The authors declare no conflict of interest.

## Copyright

© The Author(s) 2023.

## References

- [1] Suchanek W and Yoshimura M. Processing and properties of hydroxyapatite-based biomaterials for use as hard tissue replacement implants. *Journal of Materials Research*, 1998;13(1):94-117. <https://doi.org/10.1557/JMR.1998.0015>
- [2] Nayak AK. Hydroxyapatite synthesis methodologies: an overview. *International Journal of ChemTech Research*, 2010;2(2):903-907.

- [3] Wee CY, Lim QRT, Zhao Y, *et al.* Optimizing fabrication parameters via Taguchi method for production of high yield hydroxyapatite microsphere scaffolds using +Drop-on-Demand inkjet method. *Journal of Biomedical Materials Research Part B: Applied Biomaterials*, 2023;111(11):1938-1955.  
<https://doi.org/10.1002/jbm.b.35297>
- [4] Amini AR, Laurencin CT and Nukavarapu SP. Bone tissue engineering: recent advances and challenges. *Critical Reviews™ in Biomedical Engineering*, 2012;40(5):363-408.  
<https://doi.org/10.1615/CritRevBiomedEng.v40.i5.10>
- [5] Wee CY, Yang Z and Thian ES. Past, present and future development of microspheres for bone tissue regeneration: a review. *Materials Technology*, 2021;36(6):364-374.  
<https://doi.org/10.1080/10667857.2020.1759953>
- [6] Ribas RG, Schatkoski VM, do Amaral Montanheiro TL, *et al.* Current advances in bone tissue engineering concerning ceramic and bioglass scaffolds: a review. *Ceramics International*, 2019;45(17):21051-21061.  
<https://doi.org/10.1016/j.ceramint.2019.07.096>
- [7] Jeong J, Kim JH, Shim JH, *et al.* Bioactive calcium phosphate materials and applications in bone regeneration. *Biomaterials Research*, 2019;23(1):1-11.  
<https://doi.org/10.1186/s40824-018-0149-3>
- [8] Nuss KMR and von Rechenberg B. Biocompatibility issues with modern implants in bone—a review for clinical orthopedics. *The Open Orthopaedics Journal*, 2008;2:66-78.  
<https://doi.org/10.2174/1874325000802010066>
- [9] Zhang Y, Li J, Mouser VHM, *et al.* Biomimetic mechanically strong one-dimensional hydroxyapatite/poly (d, l-lactide) composite inducing formation of anisotropic collagen matrix. *ACS Nano*, 2021;15(11):17480-17498.  
<https://doi.org/10.1021/acsnano.1c03905>
- [10] Bernardo MP, da Silva BCR, Hamouda AEI, *et al.* PLA/Hydroxyapatite scaffolds exhibit in vitro immunological inertness and promote robust osteogenic differentiation of human mesenchymal stem cells without osteogenic stimuli. *Scientific Reports*, 2022;12(1):2333.  
<https://doi.org/10.1038/s41598-022-05207-w>
- [11] Shuai C, Yang W, Feng P, *et al.* Accelerated degradation of HAP/PLLA bone scaffold by PGA blending facilitates bioactivity and osteoconductivity. *Bioactive Materials*, 2021;6(2):490-502.  
<https://doi.org/10.1016/j.bioactmat.2020.09.001>
- [12] Alksne M, Kalvaityte M, Simoliunas E, *et al.* In vitro comparison of 3D printed polylactic acid/hydroxyapatite and polylactic acid/bioglass composite scaffolds: insights into materials for bone regeneration. *Journal of the Mechanical Behavior of Biomedical Materials*, 2020;104:103641.  
<https://doi.org/10.1016/j.jmbbm.2020.103641>
- [13] Moghadasi K, Isa MSM, Ariffin MA, *et al.* A review on biomedical implant materials and the effect of friction stir based techniques on their mechanical and tribological properties. *Journal of Materials Research and Technology*, 2022;17:1054-1121.  
<https://doi.org/10.1016/j.jmrt.2022.01.050>
- [14] Ripamonti U, Roden LC and Renton LF. Osteoinductive hydroxyapatite-coated titanium implants. *Biomaterials*, 2012;33(15):3813-3823.  
<https://doi.org/10.1016/j.biomaterials.2012.01.050>
- [15] Balhuc S, Campian R, Labunet A, *et al.* Dental applications of systems based on hydroxyapatite nanoparticles—an evidence-based update. *Crystals*, 2021;11(6):674.  
<https://doi.org/10.3390/cryst11060674>
- [16] O'Hagan-Wong K, Enax J, Meyer F, *et al.* The use of hydroxyapatite toothpaste to prevent dental caries. *Odontology*, 2022;110(2):223-230.  
<https://doi.org/10.1007/s10266-021-00675-4>
- [17] Akhtar K, Pervez C, Zubair N, *et al.* Calcium hydroxyapatite nanoparticles as a reinforcement filler in dental resin nanocomposite. *Journal of Materials Science: Materials in Medicine*, 2021;32:1-17.  
<https://doi.org/10.1007/s10856-021-06599-3>
- [18] Nasar A. Hydroxyapatite and its coatings in dental implants. Applications of Nanocomposite Materials in Dentistry. Amsterdam: Elsevier; 2019. p. 145-160.
- [19] Ansari Z, Kalantar M, Kharaziha M, *et al.* Polycaprolactone/fluoride substituted-hydroxyapatite (PCL/FHA) nanocomposite

- coatings prepared by in-situ sol-gel process for dental implant applications. *Progress in Organic Coatings*, 2020;147:105873.  
<https://doi.org/10.1016/j.porgcoat.2020.105873>
- [20] Zhao R, Yang R, Cooper PR, *et al.* Bone grafts and substitutes in dentistry: a review of current trends and developments. *Molecules*, 2021;26(10):3007.  
<https://doi.org/10.3390/molecules26103007>
- [21] Meyer F, Enax J, Amaechi BT, *et al.* Hydroxyapatite as remineralization agent for children's dental care. *Frontiers in Dental Medicine*, 2022;3:24.  
<https://doi.org/10.3389/fdmed.2022.859560>
- [22] Low SB, Allen EP and Kontogiorgos ED. Reduction in dental hypersensitivity with nano-hydroxyapatite, potassium nitrate, sodium monofluorophosphate and antioxidants. *The Open Dentistry Journal*, 2015;9:92-97.  
<https://doi.org/10.2174/1874364101509010092>
- [23] Anil A, Ibraheem WI, Meshni AA, *et al.* Nano-hydroxyapatite (nHAp) in the remineralization of early dental caries: a scoping review. *International Journal of Environmental Research and Public Health*, 2022;19(9):5629.  
<https://doi.org/10.3390/ijerph19095629>
- [24] Zafar MS, Khurshid Z, Najeeb S, *et al.* Therapeutic applications of nanotechnology in dentistry. In: Andronescu E, Grumezescu AM (editors). *Nanostructures for oral medicine*. Amsterdam: Elsevier; 2017. p. 833-862.
- [25] Lara-Ochoa S, Ortega-Lara W and Guerrero-Beltrán CE. Hydroxyapatite nanoparticles in drug delivery: physicochemistry and applications. *Pharmaceutics*, 2021;13(10):1642.  
<https://doi.org/10.3390/pharmaceutics13101642>
- [26] De Lama-Odría MC, Del Valle LJ and Puiggali J. Hydroxyapatite biobased materials for treatment and diagnosis of cancer. *International Journal of Molecular Sciences*, 2022;23(19):11352.  
<https://doi.org/10.3390/ijms231911352>
- [27] Xiong H, Du S, Ni J, *et al.* Mitochondria and nuclei dual-targeted heterogeneous hydroxyapatite nanoparticles for enhancing therapeutic efficacy of doxorubicin. *Biomaterials*, 2016;94:70-83.  
<https://doi.org/10.1016/j.biomaterials.2016.04.004>
- [28] Verma R, Mishra SR, Gadore V, *et al.* Hydroxyapatite-based composites: excellent materials for environmental remediation and biomedical applications. *Advances in Colloid and Interface Science*, 2023;315:102890.  
<https://doi.org/10.1016/j.cis.2023.102890>
- [29] Kong L, Mu Z, Yu Y, *et al.* Polyethyleneimine-stabilized hydroxyapatite nanoparticles modified with hyaluronic acid for targeted drug delivery. *RSC Advances*, 2016;6(104):101790-101799.  
<https://doi.org/10.1039/C6RA19351J>
- [30] Chindamo G, Sapino S, Peira E, *et al.* Bone diseases: current approach and future perspectives in drug delivery systems for bone targeted therapeutics. *Nanomaterials*, 2020;10(5):875.  
<https://doi.org/10.3390/nano10050875>
- [31] Maia ALC, Cavalcante CH, de Souza MGF, *et al.* Hydroxyapatite nanoparticles: preparation, characterization, and evaluation of their potential use in bone targeting: an animal study. *Nuclear Medicine Communications*, 2016;37(7):775-782.  
<https://doi.org/10.1097/MNM.0000000000000510>
- [32] Mo X, Zhang D, Liu K, *et al.* Nano-hydroxyapatite composite scaffolds loaded with bioactive factors and drugs for bone tissue engineering. *International Journal of Molecular Sciences*, 2023;24(2):1291.  
<https://doi.org/10.3390/ijms24021291>
- [33] Oliveira ÉR, Nie L, Podstawczyk D, *et al.* Advances in growth factor delivery for bone tissue engineering. *International Journal of Molecular Sciences*, 2021;22(2):903.  
<https://doi.org/10.3390/ijms22020903>
- [34] De Witte TM, Fratila-Apachitei LE, Zadpoor AA, *et al.* Bone tissue engineering via growth factor delivery: from scaffolds to complex matrices. *Regenerative Biomaterials*, 2018;5(4):197-211.  
<https://doi.org/10.1093/rb/rby013>
- [35] Tian J, Zhou H, Jiang R, *et al.* Preparation and biological imaging of fluorescent hydroxyapatite nanoparticles with poly (2-ethyl-2-oxazoline) through surface-initiated cationic ring-opening polymerization. *Materials Science and Engineering: C*, 2020;108:110424.  
<https://doi.org/10.1016/j.msec.2019.110424>
- [36] Bunkoed O, Donkhampa P and Nurerk P. A nanocomposite optosensor of hydroxyapatite and graphene quantum dots embedded within highly specific polymer for norfloxacin detection.



- Microchemical Journal*, 2020;158:105127.  
<https://doi.org/10.1016/j.microc.2020.105127>
- [37] Doan VHM, Vu DD, Mondal S, *et al.* Yb-Gd codoped hydroxyapatite as a potential contrast agent for tumor-targeted biomedical applications. *ACS Biomaterials Science & Engineering*, 2023;9(8):4607-4618.  
<https://doi.org/10.1021/acsbiomaterials.3c00383>
- [38] Machado TR, Leite IS, Inada NM, *et al.* Designing biocompatible and multicolor fluorescent hydroxyapatite nanoparticles for cell-imaging applications. *Materials Today Chemistry*, 2019;14:100211.  
<https://doi.org/10.1016/j.mtchem.2019.100211>
- [39] Neacsu IA, Stoica AE, Vasile BS, *et al.* Luminescent hydroxyapatite doped with rare earth elements for biomedical applications. *Nanomaterials*, 2019;9(2):239.  
<https://doi.org/10.3390/nano9020239>
- [40] Wan W, Li Z, Wang X, *et al.* Surface-fabrication of fluorescent hydroxyapatite for cancer cell imaging and bio-printing applications. *Biosensors*, 2022;12(6):419.  
<https://doi.org/10.3390/bios12060419>
- [41] Zhang N, Lu C, Chen M, *et al.* Recent advances in near-infrared II imaging technology for biological detection. *Journal of Nanobiotechnology*, 2021;19(1):132.  
<https://doi.org/10.1186/s12951-021-00870-z>
- [42] Tang W, Xu W, Zhong M, *et al.* Slightly doped hydroxyapatite pigments of subtractive color with high near-infrared reflectance. *Journal of Solid State Chemistry*, 2023;322:123947.  
<https://doi.org/10.1016/j.jssc.2023.123947>
- [43] Ashokan A, Menon D, Nair S, *et al.* A molecular receptor targeted, hydroxyapatite nanocrystal based multi-modal contrast agent. *Biomaterials*, 2010;31(9):2606-2616.  
<https://doi.org/10.1016/j.biomaterials.2009.11.113>
- [44] Zhang Q, Xiao L and Xiao Y. Porous nanomaterials targeting autophagy in bone regeneration. *Pharmaceutics*, 2021;13(10):1572.  
<https://doi.org/10.3390/pharmaceutics13101572>
- [45] Chen F, Huang P, Zhu YJ, *et al.* The photoluminescence, drug delivery and imaging properties of multifunctional Eu<sup>3+</sup>/Gd<sup>3+</sup> dual-doped hydroxyapatite nanorods. *Biomaterials*, 2011;32(34):9031-9039.  
<https://doi.org/10.1016/j.biomaterials.2011.08.032>
- [46] Bai RG, Muthoosamy K, Manickam S. Nanomedicine in theranostics. In: Thomas S, Grohens Y, Ninan N (editors). *Nanotechnology applications for tissue engineering*. Oxford: William Andrew Publishing; 2015. p. 195-213.
- [47] Lambers FM, Kuhn G and Müller R. Advances in multimodality molecular imaging of bone structure and function. *BoneKEy reports*, 2012;1:37.  
<https://doi.org/10.1038/bonekey.2012.28>
- [48] Kargozar S, Mollazadeh S, Kermani F, *et al.* Hydroxyapatite nanoparticles for improved cancer theranostics. *Journal of Functional Biomaterials*, 2022;13(3):100.  
<https://doi.org/10.3390/jfb13030100>
- [49] Villela Zumaya AL, Mincheva R, Raquez JM, *et al.* Nanocluster-based drug delivery and theranostic systems: towards cancer therapy. *Polymers*, 2022;14(6):1188.  
<https://doi.org/10.3390/polym14061188>
- [50] Jo G, Park Y, Park MH, *et al.* Near-infrared fluorescent hydroxyapatite nanoparticles for targeted photothermal cancer therapy. *Pharmaceutics*, 2023;15(5):1374.  
<https://doi.org/10.3390/pharmaceutics15051374>
- [51] Kharbikar BN, Zhong JX, Cuylear DL, *et al.* Theranostic biomaterials for tissue engineering. *Current Opinion in Biomedical Engineering*, 2021;19:100299.  
<https://doi.org/10.1016/j.cobme.2021.100299>
- [52] Kawasaki T. Hydroxyapatite as a liquid chromatographic packing. *Journal of Chromatography A*, 1991;544:147-184.  
[https://doi.org/10.1016/S0021-9673\(01\)83984-4](https://doi.org/10.1016/S0021-9673(01)83984-4)
- [53] Ashokan A, Rajendran V, Kumar TSS, *et al.* Eggshell derived hydroxyapatite microspheres for chromatographic applications by a novel dissolution-precipitation method. *Ceramics International*, 2021;47(13):18575-18583.  
<https://doi.org/10.1016/j.ceramint.2021.03.183>
- [54] Chen G, Zhitomirsky I and Ghosh R. Fast, low-pressure chromatographic separation of proteins using hydroxyapatite nanoparticles. *Talanta*, 2019;199:472-477.  
<https://doi.org/10.1016/j.talanta.2019.02.090>
- [55] Jing Y, Ding D, Tian G, *et al.* Semisynthesis of

- site-specifically succinylated histone reveals that succinylation regulates nucleosome unwrapping rate and DNA accessibility. *Nucleic Acids Research*, 2020;48(17):9538-9549.  
<https://doi.org/10.1093/nar/gkaa663>
- [56] Bahri M, Hasannia S, Dabirmanesh B, *et al.* A multifunctional fusion peptide for tethering to hydroxyapatite and selective capture of bone morphogenetic protein from extracellular milieu. *Journal of Biomedical Materials Research Part A*, 2020;108(7):1459-1466.  
<https://doi.org/10.1002/jbm.a.36915>
- [57] Gao S, Zheng M, Lin Y, *et al.* Surface-enhanced Raman scattering analysis of serum albumin via adsorption-exfoliation on hydroxyapatite nanoparticles for noninvasive cancers screening. *Journal of Biophotonics*, 2020;13(8):e202000087.  
<https://doi.org/10.1002/jbio.202000087>
- [58] Lin Y, Lin J, Zheng M, *et al.* Quantitative and direct serum albumin detection by label-free SERS using tunable hydroxyapatite nanostructure for prostate cancer detection. *Analytica Chimica Acta*, 2022;1221:340101.  
<https://doi.org/10.1016/j.aca.2022.340101>
- [59] Wang Y and Carta G. Competitive binding of monoclonal antibody monomer-dimer mixtures on ceramic hydroxyapatite. *Journal of Chromatography A*, 2019;1587:136-145.  
<https://doi.org/10.1016/j.chroma.2018.12.023>
- [60] Wang Y and Carta G. Separation of monoclonal antibody monomer-dimer mixtures by gradient elution with ceramic hydroxyapatite. *Journal of Chromatography A*, 2020;1629:461465.  
<https://doi.org/10.1016/j.chroma.2020.461465>
- [61] Alias M, Hamzah S, Saidin J, *et al.* Integration of hydroxyapatite from fish scales and polyethersulfone membrane for protease separation from *Bacillus subtilis*. *Separation Science and Technology*, 2022;57(6):910-928.  
<https://doi.org/10.1080/01496395.2021.1948866>
- [62] Fenner F, Bachmann PA, Gibbs EPJ, *et al.* Structure and composition of viruses. *Veterinary virology*. Cambridge: Academic Press; 1987. pp. 3-19.
- [63] Tleukulova Z, Stangaliyeva Z, Dildabek A, *et al.* Purification of Tomato bushy stunt virus particles by one-step hydroxyapatite column chromatography. *Eurasian Chemico-Technological Journal*, 2021;23(4):277-282.  
<https://doi.org/10.18321/ectj1131>
- [64] Kurosawa Y, Sato S, Okuyama T, *et al.* Sequential two-step chromatographic purification of infectious poliovirus using ceramic fluoroapatite and ceramic hydroxyapatite columns. *PloS One*, 2019;14(9):e0222199.  
<https://doi.org/10.1371/journal.pone.0222199>
- [65] Lin MH, Li D, Tang B, *et al.* Defective interfering particles with broad-acting antiviral activity for Dengue, Zika, Yellow Fever, Respiratory Syncytial and SARS-CoV-2 Virus infection. *Microbiology Spectrum*, 2022;10(6):e03949-22.  
<https://doi.org/10.1128/spectrum.03949-22>
- [66] Bharath G, Rambabu K, Hai A, *et al.* Synthesis of one-dimensional magnetite hydroxyapatite nanorods on reduced graphene oxide sheets for selective separation and controlled delivery of hemoglobin. *Applied Surface Science*, 2020;501:144215.  
<https://doi.org/10.1016/j.apsusc.2019.144215>
- [67] Almulaiky YQ, Khalil NM, El-Shishtawy RM, *et al.* Hydroxyapatite-decorated ZrO<sub>2</sub> for  $\alpha$ -amylase immobilization: Toward the enhancement of enzyme stability and reusability. *International Journal of Biological Macromolecules*, 2021;167:299-308.  
<https://doi.org/10.1016/j.ijbiomac.2020.11.150>
- [68] Coutinho TC, Tardioli PW and Farinas CS. Hydroxyapatite nanoparticles modified with metal ions for xylanase immobilization. *International Journal of Biological Macromolecules*, 2020;150:344-353.  
<https://doi.org/10.1016/j.ijbiomac.2020.02.058>
- [69] Coutinho TC, Malafatti JOD, Paris EC, *et al.* Hydroxyapatite-CoFe<sub>2</sub>O<sub>4</sub> magnetic nanoparticle composites for industrial enzyme immobilization, use, and recovery. *ACS Applied Nano Materials*, 2020;3(12):12334-12345.  
<https://doi.org/10.1021/acsanm.0c02811>
- [70] Yamasawa R, Saito H, Yashima Y, *et al.* Identification, characterization, and application of a d-cysteine desulfhydrase from rice seed (*Oryza sativa* L.). *Protein Expression and Purification*, 2023;211:106341.  
<https://doi.org/10.1016/j.pep.2023.106341>
- [71] Holková I, Rauová D, Mergová M, *et al.*

- Purification and product characterization of lipoxygenase from opium poppy cultures (*Papaver somniferum* L.). *Molecules*, 2019;24(23):4268. <https://doi.org/10.3390/molecules24234268>
- [72] Rohman MM, Alam SS, Akhi AH, *et al.* Response of catalase to drought in barley (*Hordeum vulgare* L.) seedlings and its purification. *African Journal of Biotechnology*, 2020;19(7):478-486. <https://doi.org/10.5897/AJB2020.17169>
- [73] Prosen H and Zupančič-Kralj L. Solid-phase microextraction. *TrAC Trends in Analytical Chemistry*, 1999;18(4):272-282. [https://doi.org/10.1016/S0165-9936\(98\)00109-5](https://doi.org/10.1016/S0165-9936(98)00109-5)
- [74] Thurman EM, Mills MS. Solid-phase extraction: principles and practice. New York: Wiley; 1998.
- [75] Wang J, Ni B, Li W, *et al.* Hydroxyapatite surface-functionalized monolithic column for selective in-tube solid phase microextraction of zoleronic acid and risedronic acid. *Journal of Chromatography A*, 2021;1653:462438. <https://doi.org/10.1016/j.chroma.2021.462438>
- [76] Wang J, Li W, Xiao J, *et al.* Hydroxyapatite-embedded monolithic column for selective on-line solid-phase extraction of adenosine triphosphate and its phosphorylated metabolites. *Journal of Chromatography B*, 2019;1128:121769. <https://doi.org/10.1016/j.jchromb.2019.121769>
- [77] Rahmani F, Hosseini MRM, Es-Haghi A, *et al.* A 96-monolithic inorganic hollow fiber array as a new geometry for high throughput solid-phase microextraction of doxorubicin in water and human urine samples coupled with liquid chromatography-tandem mass spectrometry. *Journal of Chromatography A*, 2020;1627:461413. <https://doi.org/10.1016/j.chroma.2020.461413>
- [78] Rahimpour R, Langari AAA, Alizadeh S, *et al.* Application of hydroxyapatite adsorbent packed in needle trap device for sensitive determination of trace levels of phenolic compounds in the air. *Chinese Journal of Analytical Chemistry*, 2021;49(12):27-35. <https://doi.org/10.1016/j.cjac.2021.09.008>
- [79] Bayatloo MR and Nojavan S. Rapid and simple magnetic solid-phase extraction of bisphenol A from bottled water, baby bottle, and urine samples using green magnetic hydroxyapatite/ $\beta$ -cyclodextrin polymer nanocomposite. *Microchemical Journal*, 2022;175:107180. <https://doi.org/10.1016/j.microc.2022.107180>
- [80] Lusvardi G, Malavasi G, Menabue L, *et al.* Removal of cadmium ion by means of synthetic hydroxyapatite. *Waste Management*, 2002;22(8):853-857. [https://doi.org/10.1016/S0956-053X\(02\)00078-8](https://doi.org/10.1016/S0956-053X(02)00078-8)
- [81] Hussin MSF, Abdullah HZ, Idris MI, *et al.* Extraction of natural hydroxyapatite for biomedical applications-a review. *Heliyon*, 2022;8:e10356. <https://doi.org/10.1016/j.heliyon.2022.e10356>
- [82] Wen T, Wu X, Liu M, *et al.* Efficient capture of strontium from aqueous solutions using graphene oxide-hydroxyapatite nanocomposites. *Dalton Transactions*, 2014;43(20):7464-7472. <https://doi.org/10.1039/C3DT53591F>
- [83] Xiong ZC, Zhu YJ, Wang ZY, *et al.* Tree-inspired ultralong hydroxyapatite nanowires-based multifunctional aerogel with vertically aligned channels for continuous flow catalysis, water disinfection, and solar energy-driven water purification. *Advanced Functional Materials*, 2022;32(9):2106978. <https://doi.org/10.1002/adfm.202106978>
- [84] Zhang QQ, Zhu YJ, Wu J, *et al.* Ultralong hydroxyapatite nanowire-based filter paper for high-performance water purification. *ACS Applied Materials & Interfaces*, 2019;11(4):4288-4301. <https://doi.org/10.1021/acsami.8b20703>
- [85] Koliyabandara PA, Hettithanthri O, Rathnayake A, *et al.* Hydroxyapatite for environmental remediation of water/wastewater. In: Kumar V, Kumar M (editors). *Integrated environmental technologies for wastewater treatment and sustainable development*. Amsterdam: Elsevier; 2022. p. 195-213. <https://doi.org/10.1016/B978-0-323-91180-1.00004-1>
- [86] Jung KW, Lee SY, Choi JW, *et al.* A facile one-pot hydrothermal synthesis of hydroxyapatite/biochar nanocomposites: adsorption behavior and mechanisms for the removal of copper (II) from aqueous media. *Chemical Engineering Journal*, 2019;369:529-541. <https://doi.org/10.1016/j.cej.2019.03.102>
- [87] El-Maghrabi HH, Younes AA, Salem AR, *et al.* Magnetically modified hydroxyapatite

- nanoparticles for the removal of uranium (VI): preparation, characterization and adsorption optimization. *Journal of Hazardous Materials*, 2019;378:120703.  
<https://doi.org/10.1016/j.jhazmat.2019.05.096>
- [88] Wang H, Xing H, Yan K, *et al.* Oyster shell derived hydroxyapatite microspheres as an effective adsorbent for remediation of Coomassie brilliant blue. *Advanced Powder Technology*, 2022;33(2):103425.  
<https://doi.org/10.1016/j.appt.2022.103425>
- [89] Azeez L, Adebisi SA, Adejumo AL, *et al.* Adsorptive properties of rod-shaped silver nanoparticles-functionalized biogenic hydroxyapatite for remediating methylene blue and congo red. *Inorganic Chemistry Communications*, 2022;142:109655.  
<https://doi.org/10.1016/j.inoche.2022.109655>
- [90] Chang H, Park N, Jang Y, *et al.* Application of the hydroxyapatite crystallization-filtration process to recover phosphorus from wastewater effluents. *Water Science and Technology*, 2020;81(11):2300-2310.  
<https://doi.org/10.2166/wst.2020.292>
- [91] Sun S, Gao M, Wang Y, *et al.* Phosphate removal via biological process coupling with hydroxyapatite crystallization in alternating anaerobic/aerobic biofilter reactor. *Bioresource Technology*, 2021;326:124728.  
<https://doi.org/10.1016/j.biortech.2021.124728>
- [92] Bao T, Damtie MM, Yu ZM, *et al.* Green synthesis of Fe<sub>3</sub>O<sub>4</sub>@carbon filter media for simultaneous phosphate recovery and nitrogen removal from domestic wastewater in biological aerated filters. *ACS Sustainable Chemistry & Engineering*, 2019;7(19):16698-16709.  
<https://doi.org/10.1021/acssuschemeng.9b04119>
- [93] Moreno EC, Gregory TM and Brown WE. Preparation and solubility of hydroxyapatite. *Journal of Research of the National Bureau of Standards. Section A, Physics and Chemistry*, 1968;72A(6):773-782.  
<https://doi.org/10.6028/jres.072A.052>
- [94] Tounsi H, Djemal S, Petitto C, *et al.* Copper loaded hydroxyapatite catalyst for selective catalytic reduction of nitric oxide with ammonia. *Applied Catalysis B: Environmental*, 2011;107(1-2):158-163.  
<https://doi.org/10.1016/j.apcatb.2011.07.009>
- [95] Kumar PA, Reddy MP, Ju LK, *et al.* Novel silver loaded hydroxyapatite catalyst for the selective catalytic reduction of NO<sub>x</sub> by propene. *Catalysis Letters*, 2008;126:78-83.  
<https://doi.org/10.1007/s10562-008-9561-y>
- [96] Wei X, Wang Y, Li X, *et al.* Co<sub>3</sub>O<sub>4</sub> supported on bone-derived hydroxyapatite as potential catalysts for N<sub>2</sub>O catalytic decomposition. *Molecular Catalysis*, 2020;491:111005.  
<https://doi.org/10.1016/j.mcat.2020.111005>
- [97] Shokouhimehr M, Yek SMG, Nasrollahzadeh M, *et al.* Palladium nanocatalysts on hydroxyapatite: green oxidation of alcohols and reduction of nitroarenes in water. *Applied Sciences*, 2019;9(19):4183.  
<https://doi.org/10.3390/app9194183>
- [98] Bahadorikhalili S, Arshadi H, Afrouzandeh Z, *et al.* Ultrasonic promoted synthesis of Ag nanoparticle decorated thiourea-functionalized magnetic hydroxyapatite: a robust inorganic-organic hybrid nanocatalyst for oxidation and reduction reactions. *New Journal of Chemistry*, 2020;44(21):8840-8848.  
<https://doi.org/10.1039/D0NJ00829J>
- [99] Layek K. Hydroxyapatite supported gold nanoparticles catalyzed efficient reduction of nitroarenes and degradation of azo dyes. *Catalysis Surveys from Asia*, 2023:1-14.  
<https://doi.org/10.1007/s10563-023-09401-2>
- [100] Iqbal S, ul Hassan M, Ryu HJ, *et al.* Environmentally benign and novel management route for radioactive corrosion products by hydroxyapatite. *Journal of Nuclear Materials*, 2018;507:218-225.  
<https://doi.org/10.1016/j.jnucmat.2018.05.016>
- [101] Venkatesan S, ul Hassan M and Ryu HJ. Adsorption and immobilization of radioactive ionic-corrosion-products using magnetic hydroxyapatite and cold-sintering for nuclear waste management applications. *Journal of Nuclear Materials*, 2019;514:40-49.  
<https://doi.org/10.1016/j.jnucmat.2018.11.026>
- [102] Lu K, Zhao Z, Cui J, *et al.* The immobilization of Sr (II) and Co (II) via magnetic easy-separation organophosphonate-hydroxyapatite hybrid



- nanoparticles. *Separation and Purification Technology*, 2023;315:123750.  
<https://doi.org/10.1016/j.seppur.2023.123750>
- [103] Le VT, Doan VD, Nguyen DD, *et al.* A novel cross-linked magnetic hydroxyapatite/chitosan composite: preparation, characterization, and application for Ni (II) ion removal from aqueous solution. *Water, Air, & Soil Pollution*, 2018;229:1-14.  
<https://doi.org/10.1007/s11270-018-3762-9>
- [104] Kim J, Sambudi NS and Cho K. Removal of Sr<sup>2+</sup> using high-surface-area hydroxyapatite synthesized by non-additive in-situ precipitation. *Journal of Environmental Management*, 2019;231:788-794.  
<https://doi.org/10.1016/j.jenvman.2018.10.100>
- [105] Yang K, Wang Y, Shen J, *et al.* Cs<sub>3</sub>Bi<sub>2</sub>I<sub>9</sub>-hydroxyapatite composite waste forms for cesium and iodine immobilization. *Journal of Advanced Ceramics*, 2022;11(5):712-728.  
<https://doi.org/10.1007/s40145-021-0565-z>
- [106] Skwarek E, Gładysz-Płaska A, Choromańska JB, *et al.* Adsorption of uranium ions on nano-hydroxyapatite and modified by Ca and Ag ions. *Adsorption*, 2019;25:639-647.  
<https://doi.org/10.1007/s10450-019-00063-z>
- [107] Zhou H, Xie Y, Wang X, *et al.* Efficient removal of uranium in aqueous solution by Al-doped hydroxyapatite: Static/dynamic adsorption behaviors and mechanism study. *Environmental Technology & Innovation*, 2022;25:102103.  
<https://doi.org/10.1016/j.eti.2021.102103>
- [108] Szenknect S, Mesbah A, Descostes M, *et al.* Uranium removal from mining water using Cu substituted hydroxyapatite. *Journal of Hazardous Materials*, 2020;392:122501.  
<https://doi.org/10.1016/j.jhazmat.2020.122501>
- [109] Ou T, Peng H, Su M, *et al.* Fast and efficient removal of uranium onto a magnetic hydroxyapatite composite: mechanism and process evaluation. *Processes*, 2021;9(11):1927.  
<https://doi.org/10.3390/pr9111927>
- [110] Xuan K, Wang J, Gong Z, *et al.* Hydroxyapatite modified ZIF-67 composite with abundant binding groups for the highly efficient and selective elimination of uranium (VI) from wastewater. *Journal of Hazardous Materials*, 2022;426:127834.  
<https://doi.org/10.1016/j.jhazmat.2021.127834>
- [111] Ji D, Wang Y, Liu Y, *et al.* Efficient capture of uranium by a hydroxyapatite-modified polyethyleneimine@carbon nanotube composite from radioactive nuclear waste. *Dalton Transactions*, 2023;52(29):10136-10144.  
<https://doi.org/10.1039/D3DT01810E>
- [112] Saha S, Basu H, Rout S, *et al.* Nano-hydroxyapatite coated activated carbon impregnated alginate: a new hybrid sorbent for uranium removal from potable water. *Journal of Environmental Chemical Engineering*, 2020;8(4):103999.  
<https://doi.org/10.1016/j.jece.2020.103999>
- [113] Liao J, Xiong T, Ding L, *et al.* Design of a renewable hydroxyapatite-biocarbon composite for the removal of uranium (VI) with high-efficiency adsorption performance. *Biochar*, 2022;4(1):29.  
<https://doi.org/10.1007/s42773-022-00154-1>
- [114] Ahmed W, Núñez-Delgado A, Mehmood S, *et al.* Highly efficient uranium (VI) capture from aqueous solution by means of a hydroxyapatite-biochar nanocomposite: Adsorption behavior and mechanism. *Environmental Research*, 2021;201:111518.  
<https://doi.org/10.1016/j.envres.2021.111518>
- [115] Su M, Tsang DCW, Ren X, *et al.* Removal of U (VI) from nuclear mining effluent by porous hydroxyapatite: evaluation on characteristics, mechanisms and performance. *Environmental Pollution*, 2019;254:112891.  
<https://doi.org/10.1016/j.envpol.2019.07.059>
- [116] Wu Y, Chen D, Kong L, *et al.* Rapid and effective removal of uranium (VI) from aqueous solution by facile synthesized hierarchical hollow hydroxyapatite microspheres. *Journal of Hazardous Materials*, 2019;371:397-405.  
<https://doi.org/10.1016/j.jhazmat.2019.02.110>
- [117] Ma C, Su M, Song G, *et al.* Fabrication of highly efficient hydroxyapatite microtubes for uranium sequestration and immobilization. *Journal of Environmental Management*, 2023;344:118417.  
<https://doi.org/10.1016/j.jenvman.2023.118417>
- [118] Xiong T, Li Q, Liao J, *et al.* Highly enhanced adsorption performance to uranium (VI) by facile synthesized hydroxyapatite aerogel. *Journal of*

- Hazardous Materials*, 2022;423:127184.  
<https://doi.org/10.1016/j.jhazmat.2021.127184>
- [119] Huang S, Chen C, Zhao Z, *et al.* Highly efficient separation of uranium from wastewater by in situ synthesized hydroxyapatite modified coal fly ash composite aerogel. *Journal of Industrial and Engineering Chemistry*, 2023;118:418-431.  
<https://doi.org/10.1016/j.jiec.2022.11.026>
- [120] Xiong T, Li Q, Liao J, *et al.* Design of hydroxyapatite aerogel with excellent adsorption performance to uranium. *Journal of Environmental Chemical Engineering*, 2021;9(6):106364.  
<https://doi.org/10.1016/j.jece.2021.106364>
- [121] Wang Y, Chen B, Xiong T, *et al.* Highly efficient uranium capture from wastewater by hydroxyapatite aerogels prepared with konjac gum as template. *Journal of Water Process Engineering*, 2022;48:102919.  
<https://doi.org/10.1016/j.jwpe.2022.102919>
- [122] Xiong T, Jia L, Li Q, *et al.* Efficient removal of uranium by hydroxyapatite modified kaolin aerogel. *Separation and Purification Technology*, 2022;299:121776.  
<https://doi.org/10.1016/j.seppur.2022.121776>
- [123] Park JH, Lee GD, Nishikata A, *et al.* Anticorrosive behavior of hydroxyapatite as an environmentally friendly pigment. *Corrosion Science*, 2002;44(5):1087-1095.  
[https://doi.org/10.1016/S0010-938X\(01\)00118-4](https://doi.org/10.1016/S0010-938X(01)00118-4)
- [124] Guo XJ, Yuan XY, Zhao SR, *et al.* Improving anticorrosion performance of hydroxyapatite via controlling exposed crystal surface and applications. *Journal of Alloys and Compounds*, 2020;845:156290.  
<https://doi.org/10.1016/j.jallcom.2020.156290>
- [125] Cheng L, Wu H, Li J, *et al.* Polydopamine modified ultrathin hydroxyapatite nanosheets for anti-corrosion reinforcement in polymeric coatings. *Corrosion Science*, 2021;178:109064.  
<https://doi.org/10.1016/j.corsci.2020.109064>
- [126] Zhou Z, Zheng B, Gu Y, *et al.* New approach for improving anticorrosion and biocompatibility of magnesium alloys via polydopamine intermediate layer-induced hydroxyapatite coating. *Surfaces and Interfaces*, 2020;19:100501.  
<https://doi.org/10.1016/j.surf.2020.100501>
- [127] Guo Y, Yu Z, Chen L, *et al.* Preparation and performance of a composite epoxy coating based on modified hydroxyapatite. *Surface and Coatings Technology*, 2022;443:128614.  
<https://doi.org/10.1016/j.surfcoat.2022.128614>
- [128] Xu X, Wang H, Wu J, *et al.* Hydrothermal in-situ synthesis and anti-corrosion performance of zinc oxide hydroxyapatite nanocomposite anti-corrosive pigment. *Coatings*, 2022;12(4):420.  
<https://doi.org/10.3390/coatings12040420>
- [129] Xue XZ, Zhang JY, Zhou D, *et al.* In-situ bonding technology and excellent anticorrosion activity of graphene oxide/hydroxyapatite nanocomposite pigment. *Dyes and Pigments*, 2019;160:109-118.  
<https://doi.org/10.1016/j.dyepig.2018.07.057>
- [130] Predoi D, Popa CL, Chapon P, *et al.* Evaluation of the antimicrobial activity of different antibiotics enhanced with silver-doped hydroxyapatite thin films. *Materials*, 2016;9(9):778.  
<https://doi.org/10.3390/ma9090778>
- [131] Trentin DS, Silva DB, Frasson AP, *et al.* Natural green coating inhibits adhesion of clinically important bacteria. *Scientific Reports*, 2015;5(1):8287.  
<https://doi.org/10.1038/srep08287>
- [132] Sinulingga K, Sirait M, Siregar N, *et al.* Investigation of antibacterial activity and cell viability of Ag/Mg and Ag/Zn co-doped hydroxyapatite derived from natural limestone. *ACS Omega*, 2021;6(49):34185-34191.  
<https://doi.org/10.1021/acsomega.1c05921>
- [133] Esmaeili Y, Zamindar N and Mohammadi R. The effect of polypropylene film containing nano-hydroxyapatite on Physicochemical and microbiological properties of button mushrooms (*Agaricus bisporus*) under Modified atmosphere packaging. *Journal of Food Measurement and Characterization*, 2023;17(1):773-786.  
<https://doi.org/10.1007/s11694-022-01613-w>
- [134] Yin IX, Zhang J, Zhao IS, *et al.* The antibacterial mechanism of silver nanoparticles and its application in dentistry. *International Journal of Nanomedicine*, 2020;15:2555-2562.  
<https://doi.org/10.2147/IJN.S246764>
- [135] Feng QL, Wu J, Chen GQ, *et al.* A mechanistic study of the antibacterial effect of silver ions on *Escherichia coli* and *Staphylococcus aureus*. *Journal of Biomedical Materials Research*,

- 2000;52(4):662-668.
- [136] Gökmen FÖ. Hydroxyapatite-doped polyhydroxyethylmethacrylate hydrogels as smart porous packaging materials. *Food and Bioprocess Technology*, 2023;16:2692-2704.  
<https://doi.org/10.1007/s11947-023-03097-y>
- [137] Malvano F, Montone AMI, Capparelli R, *et al.* Development of a novel active edible coating containing hydroxyapatite for food shelf-life extension. *Chemical Engineering Transactions*, 2021;87:25-30.  
<https://doi.org/10.3303/CET2187005>
- [138] Malvano F, Montone AMI, Capuano F, *et al.* Effects of active alginate edible coating enriched with hydroxyapatite-quercetin complexes during the cold storage of fresh chicken fillets. *Food Packaging and Shelf Life*, 2022;32:100847.  
<https://doi.org/10.1016/j.fpsl.2022.100847>
- [139] Wang Y, Cheng M, Yan X, *et al.* Preparation and characterization of an active packaging film loaded with tea tree oil-hydroxyapatite porous microspheres. *Industrial Crops and Products*, 2023;199:116783.  
<https://doi.org/10.1016/j.indcrop.2023.116783>
- [140] Akaki T, Maehara H and Tooyama M. Development of wood and wood ash-based hydroxyapatite composites and their fire-retarding properties. *Journal of Wood Science*, 2012;58(6):532-537.  
<https://doi.org/10.1007/s10086-012-1276-4>
- [141] Tonsuaadu K, Gross KA, Plūduma L, *et al.* A review on the thermal stability of calcium apatites. *Journal of Thermal Analysis and Calorimetry*, 2012;110(2):647-659.  
<https://doi.org/10.1007/s10973-011-1877-y>
- [142] Zhu YJ. Multifunctional fire-resistant paper based on ultralong hydroxyapatite nanowires. *Chinese Journal of Chemistry*, 2021;39(8):2296-2314.  
<https://doi.org/10.1002/cjoc.202100170>
- [143] Chen FF, Zhu YJ, Chen F, *et al.* Fire alarm wallpaper based on fire-resistant hydroxyapatite nanowire inorganic paper and graphene oxide thermosensitive sensor. *ACS Nano*, 2018;12(4):3159-3171.  
<https://doi.org/10.1021/acsnano.8b00047>
- [144] Vahabi H, Gholami F, Karaseva V, *et al.* Novel nanocomposites based on poly (ethylene-co-vinyl acetate) for coating applications: the complementary actions of hydroxyapatite, MWCNTs and ammonium polyphosphate on flame retardancy. *Progress in Organic Coatings*, 2017;113:207-217.  
<https://doi.org/10.1016/j.porgcoat.2017.08.009>
- [145] Ai J, Guo Z and Liu W. Superamphiphobic coatings with antifouling and nonflammable properties using functionalized hydroxyapatite. *New Journal of Chemistry*, 2021;45(14):6238-6246.  
<https://doi.org/10.1039/D1NJ00277E>
- [146] Członka S, Kairyte A, Miedzińska K, *et al.* Polyurethane hybrid composites reinforced with lavender residue functionalized with kaolinite and hydroxyapatite. *Materials*, 2021;14(2):415.  
<https://doi.org/10.3390/ma14020415>
- [147] Nihmath A and Ramesan MT. Studies on the role of hydroxyapatite nanoparticles in imparting unique thermal, dielectric, flame retardancy and petroleum fuel resistance to novel chlorinated EPDM/chlorinated NBR blend. *Research on Chemical Intermediates*, 2020;46(11):5049-5068.  
<https://doi.org/10.1007/s11164-020-04239-z>
- [148] Zhou Y, Qiu S, Ding L, *et al.* Innovative design of environmentally friendly silicon-based polyphosphazene-functionalized hydroxyapatite nanowires: an efficient enhancement strategy for the fire safety and mechanical properties of unsaturated polyester. *Chemical Engineering Journal*, 2022;437:135489.  
<https://doi.org/10.1016/j.cej.2022.135489>
- [149] Huang Q, Xue H, Dong R, *et al.* Simple and green synthesis of calcium alginate/hydroxyapatite hybrid material without high temperature treatment and its flame retardancy. *Cellulose*, 2022;29(3):1759-1774.  
<https://doi.org/10.1007/s10570-021-04373-w>
- [150] Zhu J, Li X, Li D, *et al.* Thermal insulation and flame retardancy of the hydroxyapatite nanorods/sodium alginate composite aerogel with a double-crosslinked structure. *ACS Applied Materials & Interfaces*, 2022;14(40):45822-45831.  
<https://doi.org/10.1021/acsnano.2c12254>
- [151] Zhu J, Xiong R, Zhao F, *et al.* Lightweight, high-strength, and anisotropic structure composite aerogel based on hydroxyapatite nanocrystal

- and chitosan with thermal insulation and flame retardant properties. *ACS Sustainable Chemistry & Engineering*, 2019;8(1):71-83.  
<https://doi.org/10.1021/acssuschemeng.9b03953>
- [152] Nabipour H, Wang X, Song L, *et al.* A fully bio-based coating made from alginate, chitosan and hydroxyapatite for protecting flexible polyurethane foam from fire. *Carbohydrate Polymers*, 2020;246:116641.  
<https://doi.org/10.1016/j.carbpol.2020.116641>
- [153] Wang ZY, Zhu YJ, Chen YQ, *et al.* Flexible nanocomposite paper with superior fire retardance, mechanical properties and electrical insulation by engineering ultralong hydroxyapatite nanowires and aramid nanofibers. *Chemical Engineering Journal*, 2022;444:136470.  
<https://doi.org/10.1016/j.cej.2022.136470>
- [154] Huang J, E S, Si L, *et al.* Composite films of hydroxyethyl cellulose and hydroxyapatite nanowires with high mechanical strength and electrical insulation property. *Journal of Wood Chemistry and Technology*, 2022;42(1):15-25.  
<https://doi.org/10.1080/02773813.2021.1998128>
- [155] Dong LY, Zhu YJ and Wu J. Wet end chemical properties of a new kind of fire-resistant paper pulp based on ultralong hydroxyapatite nanowires. *Molecules*, 2022;27(20):6808.  
<https://doi.org/10.3390/molecules27206808>
- [156] Li H, Wu D, Wu J, *et al.* Flexible, high-wettability and fire-resistant separators based on hydroxyapatite nanowires for advanced lithium-ion batteries. *Advanced Materials*, 2017;29(44):1703548.  
<https://doi.org/10.1002/adma.201703548>
- [157] Wen J, Zhang R, Zhao Q, *et al.* Hydroxyapatite nanowire-reinforced poly (ethylene oxide)-based polymer solid electrolyte for application in high-temperature lithium batteries. *ACS Applied Materials & Interfaces*, 2020;12(49):54637-54643.  
<https://doi.org/10.1021/acsaami.0c15692>
- [158] Liang Y, Liu Y, Chen D, *et al.* Hydroxyapatite functionalization of solid polymer electrolytes for high-conductivity solid-state lithium-ion batteries. *Materials Today Energy*, 2021;20:100694.  
<https://doi.org/10.1016/j.mtener.2021.100694>
- [159] Xi C, Cui X, Zhang R, *et al.* Utilizing an oxygen-rich interface by hydroxyapatite to regulate the linear diffusion for the stable solid-state electrolytes. *ACS Applied Materials & Interfaces*, 2022;14(29):33392-33399.  
<https://doi.org/10.1021/acsaami.2c09207>
- [160] Rao Z, Yang Z, Gong W, *et al.* Simultaneously suppressing lithium dendrite growth and Mn dissolution by integration of a safe inorganic separator in a LiMn<sub>2</sub>O<sub>4</sub>/Li battery. *Journal of Materials Chemistry A*, 2020;8(7):3859-3864.  
<https://doi.org/10.1039/C9TA12979K>
- [161] Li R, Sun X, Zou J, *et al.* Hydroxyapatite nanowires composite interlayer based on aramid fiber paper for Li-S batteries. *Journal of Electroanalytical Chemistry*, 2020;856:113662.  
<https://doi.org/10.1016/j.jelechem.2019.113662>
- [162] Wang JY, Tong XF, Peng QF, *et al.* Efficient interface enabled by nano-hydroxyapatite@porous carbon for lithium-sulfur batteries. *Journal of Electrochemistry*, 2022;28(11):2219008.
- [163] Saroja APVK, Kumar A, Moharana BC, *et al.* Design of porous calcium phosphate based gel polymer electrolyte for quasi-solid state sodium ion battery. *Journal of Electroanalytical Chemistry*, 2020;859:113864.  
<https://doi.org/10.1016/j.jelechem.2020.113864>
- [164] Rao Z, Meng J, Wu J, *et al.* A multifunctional inorganic composite separator for stable high-safety lithium-sulfur batteries. *ACS Applied Energy Materials*, 2020;3(10):10139-10146.  
<https://doi.org/10.1021/acsaem.0c01842>
- [165] Hou Y, Huang Z, Chen Z, *et al.* Bifunctional separators design for safe lithium-ion batteries: suppressed lithium dendrites and fire retardance. *Nano Energy*, 2022;97:107204.  
<https://doi.org/10.1016/j.nanoen.2022.107204>
- [166] Liu Y, Li C, Li C, *et al.* Highly thermally stable, highly electrolyte-wettable hydroxyapatite/cellulose nanofiber hybrid separators for lithium-ion batteries. *ACS Applied Energy Materials*, 2023;6(7):3862-3871.  
<https://doi.org/10.1021/acsaem.2c04170>
- [167] Chen W, Wang X, Liang J, *et al.* A high performance polyacrylonitrile composite separator with cellulose acetate and nano-hydroxyapatite for lithium-ion batteries. *Membranes*, 2022;12(2):124.  
<https://doi.org/10.3390/membranes12020124>



- [168] Selvam S and Yim JH. High temperature-functioning ceramic-based ionic liquid electrolyte engraved planar HAp/PVP/MnO<sub>2</sub>@MnCO<sub>3</sub> supercapacitors on carbon cloth. *Journal of Materials Chemistry A*, 2021;9(25):14319-14330. <https://doi.org/10.1039/D0TA11980F>
- [169] Eswaran M, Swamiappan S, Chokkiah B, *et al.* A green and economical approach to derive nanostructured hydroxyapatite from Garra mullya fish scale waste for biocompatible energy storage applications. *Materials Letters*, 2021;302:130341. <https://doi.org/10.1016/j.matlet.2021.130341>
- [170] Chu M, Zhai Y, Shang N, *et al.* Functions of hydroxyapatite in fabricating N-doped carbon for excellent catalysts and supercapacitors. *Catalysis Science & Technology*, 2019;9(18):4952-4960. <https://doi.org/10.1039/C9CY00804G>
- [171] Chu M, Zhai Y, Shang N, *et al.* N-doped carbon derived from the monomer of chitin for high-performance supercapacitor. *Applied Surface Science*, 2020;517:146140. <https://doi.org/10.1016/j.apsusc.2020.146140>
- [172] Lv S, Ma L, Zhou Q, *et al.* One-step pyrolysis toward nitrogen-doped hierarchical porous carbons for supercapacitors. *Journal of Materials Science*, 2020;55:12191-12202. <https://doi.org/10.1007/s10853-020-04876-0>
- [173] Li WC, Chen RK and Wen TC. The role of nano-hydroxyapatite bearing zwitterion within carboxylated chitosan hydrogel electrolyte in improving supercapacitor performance. *Electrochimica Acta*, 2023;466:143064. <https://doi.org/10.1016/j.electacta.2023.143064>
- [174] Roveri N, Falini G, Sidoti MC, *et al.* Biologically inspired growth of hydroxyapatite nanocrystals inside self-assembled collagen fibers. *Materials Science and Engineering: C*, 2003;23(3):441-446. [https://doi.org/10.1016/S0928-4931\(02\)00318-1](https://doi.org/10.1016/S0928-4931(02)00318-1)
- [175] Sadek H, Siddique SK, Wang CW, *et al.* Bioinspired nanonetwork hydroxyapatite from block copolymer templated synthesis for mechanical metamaterials. *ACS Nano*, 2022;16(11):18298-18306. <https://doi.org/10.1021/acsnano.2c06040>
- [176] Bai H, Walsh F, Gludovatz B, *et al.* Bioinspired hydroxyapatite/poly (methyl methacrylate) composite with a nacre-mimetic architecture by a bidirectional freezing method. *Advanced Materials*, 2016;28(1):50-56. <https://doi.org/10.1002/adma.201504313>
- [177] Qi Y, Cheng Z, Ye Z, *et al.* Bioinspired mineralization with hydroxyapatite and hierarchical naturally aligned nanofibrillar cellulose. *ACS Applied Materials & Interfaces*, 2019;11(31):27598-27604. <https://doi.org/10.1021/acsami.9b09443>
- [178] Huang C, Fang G, Zhao Y, *et al.* Bio-inspired nanocomposite by layer-by-layer coating of chitosan/hyaluronic acid multilayers on a hard nanocellulose-hydroxyapatite matrix. *Carbohydrate Polymers*, 2019;222:115036. <https://doi.org/10.1016/j.carbpol.2019.115036>
- [179] Wan F, Ping H, Wang W, *et al.* Hydroxyapatite-reinforced alginate fibers with bioinspired dually aligned architectures. *Carbohydrate Polymers*, 2021;267:118167. <https://doi.org/10.1016/j.carbpol.2021.118167>
- [180] Gomez-Vazquez OM, Correa-Piña BA, Zubietta-Otero LF, *et al.* Synthesis and characterization of bioinspired nano-hydroxyapatite by wet chemical precipitation. *Ceramics International*, 2021;47(23):32775-32785. <https://doi.org/10.1016/j.ceramint.2021.08.174>
- [181] Fu XK, Cao HB, An YL, *et al.* Bioinspired hydroxyapatite coating infiltrated with a graphene oxide hybrid supramolecular hydrogel orchestrates antibacterial and self-lubricating performance. *ACS Applied Materials & Interfaces*, 2022;14(28):31702-31714. <https://doi.org/10.1021/acsami.2c07869>
- [182] Mu Y, Feng H, Zhang S, *et al.* Development of highly permeable and antifouling ultrafiltration membranes based on the synergistic effect of carboxylated polysulfone and bio-inspired co-deposition modified hydroxyapatite nanotubes. *Journal of Colloid and Interface Science*, 2020;572:48-61. <https://doi.org/10.1016/j.jcis.2020.03.072>
- [183] Shao CS, Chen LJ, Tang RM, *et al.* Polarized hydroxyapatite/BaTiO<sub>3</sub> scaffolds with bio-inspired porous structure for enhanced bone penetration. *Rare Metals*, 2022;41(1):67-77. <https://doi.org/10.1007/s12598-021-01798-x>
- [184] Platini M, Ropars T, Pelletier B, *et al.* CPU

- overheating prediction in HPC systems. *Concurrency and Computation: Practice and Experience*, 2021;33(13):e6231. <https://doi.org/10.1002/cpe.6231>
- [185] Lee M and Kim H. COVID-19 pandemic and microplastic pollution. *Nanomaterials*, 2022;12(5):851. <https://doi.org/10.3390/nano12050851>
- [186] Romagnoli L and Fanelli RM. Annual food waste per capita as influenced by geographical variations. *Rivista Di Studi Sulla Sostenibilità*, 2019. pp. 59-76.